Cross talk between Wnt/β–catenin and *Irf8* in leukemia progression and drug resistance

Marina Scheller,[1,2] Jörg Schönheit,[1] Karin Zimmermann,[3] Ulf Leser,[3] Frank Rosenbauer,[4] and Achim Leutz[1,2]

[1]Max Delbrück Center for Molecular Medicine, 13125 Berlin, Germany
[2]Berlin-Brandenburg Center for Regenerative Therapies, Charité-Universitätsmedizin Berlin, 13353 Berlin, Germany
[3]Institute for Computer Science, Humboldt-University of Berlin, 10099 Berlin, Germany
[4]Institute of Molecular Tumor Biology, Medical Faculty of the University of Muenster, 48149 Muenster, Germany

Progression and disease relapse of chronic myeloid leukemia (CML) depends on leukemia-initiating cells (LIC) that resist treatment. Using mouse genetics and a BCR–ABL model of CML, we observed cross talk between Wnt/β–catenin signaling and the *interferon-regulatory factor 8* (*Irf8*). In normal hematopoiesis, activation of β–catenin results in up-regulation of *Irf8*, which in turn limits oncogenic β–catenin functions. Self-renewal and myeloproliferation become dependent on β–catenin in *Irf8*-deficient animals that develop a CML-like disease. Combined *Irf8* deletion and constitutive β–catenin activation result in progression of CML into fatal blast crisis, elevated leukemic potential of BCR–ABL–induced LICs, and Imatinib resistance. Interestingly, activated β–catenin enhances a preexisting *Irf8*-deficient gene signature, identifying β–catenin as an amplifier of progression-specific gene regulation in the shift of CML to blast crisis. Collectively, our data uncover *Irf8* as a roadblock for β–catenin–driven leukemia and imply both factors as targets in combinatorial therapy.

CORRESPONDENCE
Achim Leutz:
aleutz@mdc-berlin.de
OR
Marina Scheller:
m.scheller@uke.de

Abbreviations used: 4-OHT, 4-hydroxy-tamoxifen; APC, allophycocyanin; BMT, BM transplantation; BP, blast-crisis phase; CML, chronic myeloid leukemia; CMP, common myeloid progenitor; CP, chronic phase; dpi, days post injection; EMSA, electrophoretic mobility shift assay; GMP, granulocyte/monocyte progenitor; HSC, hematopoietic stem cell; *Irf8*, *IFN-regulatory factor 8*; LIC, leukemia-initiating cell; LSK, lineage-negative Sca-1^{+} c-Kit[+]; MEP, megakaryocyte/erythrocyte progenitor; PSS, progression-specific signature; SP, side population; TBE, Tcf/Lef1-binding element; TKI, tyrosine kinase inhibitor.

Chronic myeloid leukemia (CML) is a clonal myeloproliferative disorder that results from the stable recurrent Philadelphia chromosomal translocation (Ph[+]) in hematopoietic stem cells (HSCs), giving rise to the oncogenic BCR-ABL fusion protein (Nowell and Hungerford, 1960; Bartram et al., 1983). The course of CML is biphasic, with a prolonged chronic phase (CP) that eventually progresses to a fatal blast-crisis phase (BP) that is characterized by accumulation of differentiation-arrested and therapy-resistant blast cells (Perrotti et al., 2010). Administration of BCR-ABL tyrosine kinase inhibitors (TKIs) can efficiently restrain CML-CP, but complete remission is difficult to achieve due to persistence of TKI-resistant leukemia-initiating cells (LICs) that may reestablish CML and cause disease relapse (Druker et al., 2006; Crews and Jamieson, 2013). These observations highlight the clinical need to approach mechanisms of CML LIC's persistence.

The presence of putative LICs in different types of leukemia and their clinical relevance has been determined experimentally (Bonnet and Dick, 1997; Eppert et al., 2011). LICs may originate from normal HSCs or from committed progenitors that share a core transcriptional "stemness" program with HSCs (Krivtsov et al., 2006; Eppert et al., 2011). Wnt/β–catenin signaling is one of the important players in the stem cell pathways. Although the role of Wnt/β–catenin signaling in the regulation of self-renewal in normal HSCs remains under debate (Cobas et al., 2004; Jeannet et al., 2008; Koch et al., 2008), its involvement in leukemogenesis and necessity for development of LICs is widely acknowledged (Müller-Tidow et al., 2004; Malhotra and Kincade, 2009; Wang et al., 2010; Yeung et al., 2010; Luis et al., 2012). In BCR–ABL–induced CML, Wnt/β–catenin signaling is aberrantly activated and responsible for expanding the granulocyte/monocyte progenitor (GMP) pool in patients with blast crisis (Jamieson et al., 2004; Abrahamsson et al., 2009). Although deletion of β–catenin in a BCR–ABL–induced CML mouse model led to impaired leukemogenesis (Zhao et al., 2007; Hu et al., 2009), delay of disease recurrence and abrogation of fully developed

The Rockefeller University Press $30.00
J. Exp. Med. 2013 Vol. 210 No. 11 2239–2256
www.jem.org/cgi/doi/10.1084/jem.20130706

2239

CML LICs were only achieved with Imatinib cotreatment (Heidel et al., 2012). These studies suggested that canonical Wnt signaling could become a druggable target in patients with minimal residual CML disease (Heidel et al., 2012).

Another recurrent lesion in CML pathogenesis involves the *IFN-regulatory factor 8* (*Irf8*), which has been established as a tumor suppressor in CML (Holtschke et al., 1996; Hao and Ren, 2000; Deng and Daley, 2001; Tamura et al., 2003; Burchert et al., 2004). Patients with CML show reduced *Irf8* expression, and successful CML therapy is associated with a restoration of *Irf8* level (Schmidt et al., 1998). Targeted deletion of *Irf8* in the mouse leads to development of a CML-like disease (Holtschke et al., 1996; Scheller et al., 1999). Downregulation of *Irf8* is required for murine BCR-ABL–inducible CML disease, whereas coexpression of *Irf8* repressed the mitogenic activity of BCR-ABL in vivo (Hao and Ren, 2000) and in vitro (Tamura et al., 2003; Burchert et al., 2004). Loss of *Irf8* synergized with different oncogenes and induced myeloblastic transformation (Schwieger et al., 2002; Gurevich et al., 2006; Hara et al., 2008); however, progression of *Irf8*$^{-/-}$ CML-like disease in mice occurred rarely and only after long latency (Holtschke et al., 1996). These results suggested that *Irf8* deficiency is a prerequisite but not sufficient for malignant transformation and requires an additional genetic lesion for blast crisis progression.

Irf8 functions as an anti-oncoprotein that inhibits expression of *myc*, an important target gene of BCR-ABL (Tamura et al., 2003), negatively controls anti-apoptotic genes, such as *bcl2*, *bcl2l1* (*bcl-xl*), or *Ptpn13* (Fas-associated phosphatase-1), and enhances the expression of proapoptotic genes, such as caspase-3 (Gabriele et al., 1999; Burchert et al., 2004). Recent studies have also suggested a link between *Irf8* deficiency and increased expression and activity of β-catenin that may associate with poor prognosis and CML-BP transition (Huang et al., 2010).

In this study, we demonstrate that cross talk between canonical Wnt and IFN signaling determines development of CML-LICs and represents a BCR-ABL–independent mechanism of disease progression underlying the acquisition of resistance to Imatinib at later stages of CML. Because elimination of β-catenin did not affect normal HSCs and because *Irf8* antagonized BCR-ABL–induced leukemia, targeting of both pathways together with TKI treatment may pave the way to more effective combinatorial therapeutic strategies in the treatment of advanced CML.

RESULTS
Irf8 is a functional downstream target of β-catenin

Activation of Wnt/β-catenin signaling in the hematopoietic system of mice has previously been shown to result in impaired lineage differentiation and rapid death of the animals (Kirstetter et al., 2006; Scheller et al., 2006). Gene expression profiling was now used to explore consequences of β-catenin activation in the HSC enriched lineage-negative (Lin$^-$) Sca-1$^+$ c-Kit$^+$ (LSK) bone marrow compartment, using MxCre$^+$ *Ctnnb1*$^{(Ex3)fl/+}$ and control MxCre$^-$ *Ctnnb1*$^{(Ex3)fl/+}$ mice. As

shown in Fig. 1 A, β-catenin activation led to up-regulation of proapoptotic and down-regulation of prosurvival genes that was also noted by others (Perry et al., 2011). Remarkably, genes associated with self-renewal and leukemogenesis, such as *Meis1*, *Hoxa9*, *Runx2*, *Mef2c*, and *Mylk*, were transcriptionally down-regulated. Using established myeloid (GM)- and erythroid (E)-specific gene signatures (Månsson et al., 2007), we found that in *Ctnnb1*$^{(Ex3)\Delta/+}$ LSK cells, E-specific gene expression was increased (e.g., *Gata1*, *Ermap*, *Klf1*, *Pklr*, and *Epor*), whereas myeloid gene expression (e.g., *Elane*, *Csf1r*, *Csf3*, *Mpo*, and *Cebpa*) was diminished, mirroring the prospective lineage commitment defect.

Expression of key transcription factors that orchestrate myeloid differentiation (Rosenbauer and Tenen, 2007) was validated by RT-PCR. Expression of *Sfpi1* (*Pu.1*) and *Cebpa* mRNAs was strongly reduced and expression of *Irf8* was up-regulated (Fig. 1 B). Enhanced Irf8 expression was also evident by protein analysis (Fig. 1 C) and was consistent with the enrichment of *Irf8* target genes (Tamura et al., 2005; Kubosaki et al., 2010) in the *Ctnnb1*$^{(Ex3)\Delta/+}$ LSK gene expression signature (Fig. 1 D). Analysis of the *Irf8* promoter region revealed three consensus-binding sites for the β-catenin target transcription factors Tcf/Lef1 (Tcf/Lef1-binding elements [TBEs], CTTTGAT and ATCAAAG, respectively) in a region 1.7 kb upstream of the transcriptional start site (Fig. 1 E). A β-catenin/Lef1 construct enhanced *Irf8* promoter (−1710 to +33)–driven reporter expression in a TBE2 site-dependent fashion (Fig. 1 F). Electrophoretic mobility shift assays (EMSAs) confirmed binding of β-catenin/Lef1 to the TBE2 site (Fig. 1 G). These results identify *Irf8* as a novel Wnt/β-catenin target gene.

To explore the functional consequences of *Irf8* up-regulation on myeloid lineage commitment of *Ctnnb1*$^{(Ex3)\Delta/+}$ LSK cells, WT HSC- and progenitor-enriched Lin$^-$ BM cells were transduced with a retroviral construct carrying *Irf8* cDNA or 4-hydroxy-tamoxifen (4-OHT)–inducible *Irf8* (*Irf8*-ER^{T2}) and analyzed in CFU assays and by transplantation into lethally irradiated mice. Induction of *Irf8* reduced the percentage of myeloid GFP$^+$CD11b$^+$ cells in animals (Fig. 1 H, top), while GFP$^+$B220$^+$ B cells remained constant (Fig. 1 H, bottom). Analysis of apoptosis showed increased Annexin V staining within the myeloid compartment (GFP$^+$CD11b$^+$), but not in B cells (GFP$^+$B220$^+$ cells; unpublished data). Furthermore, enforced expression of *Irf8* reduced myeloid colony formation, in particular granulocyte-monocyte (GM)– and granulocyte (G)-CFUs (Fig. 1 I). In accordance with previous findings, expression of a stabilized form of β-catenin also reduced colony formation (Fig. 1 I). In a reciprocal experiment, a stabilized β-catenin construct was introduced into *Irf8*$^{-/-}$ progenitors. In contrast to the WT cells, introduction of stabilized β-catenin into *Irf8*-deficient Lin$^-$ BMCs barely affected proliferation and colony formation (Fig. 1 J). Altogether, constitutive activation of Wnt/β-catenin signaling in HSCs resulted in repression of self-renewal–associated genes, increased apoptosis, and altered lineage priming that may provide the explanation for early lethality of mice after β-catenin activation.
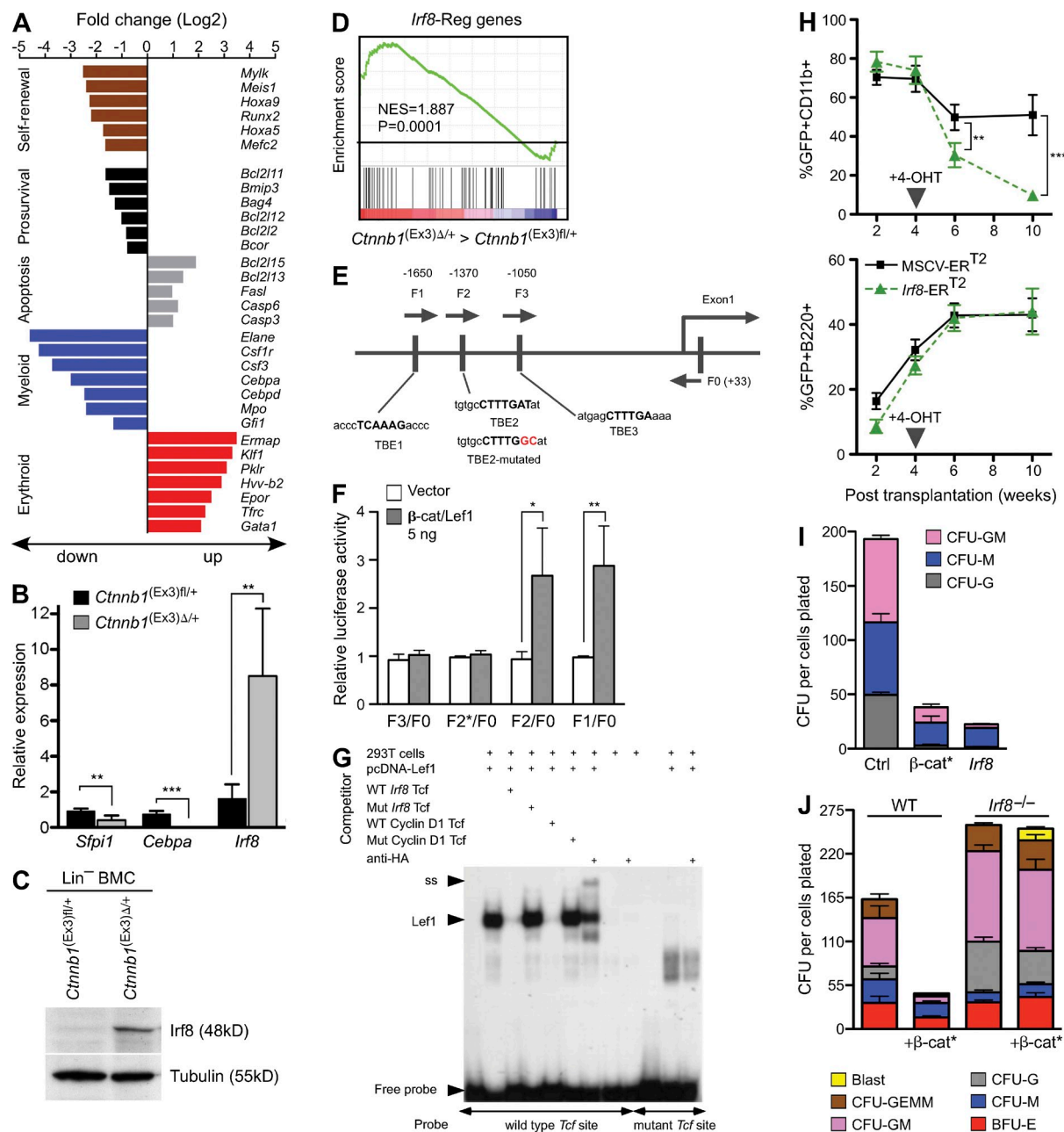
Figure 1. *Irf8* **is a downstream effector of activated β–catenin and restrains myeloid development.** (A) Alteration of gene expression after β-catenin activation in HSC. Overview of selected differential gene expression patterns in sorted LSKs from MxCre+*Ctnnb1*(Ex3)Δ/+ (denoted *Ctnnb1*(Ex3)Δ/+; Δ, deleted) compared with control MxCre−*Ctnnb1*(Ex3)fl/+ (denoted *Ctnnb1*(Ex3)fl/+; fl, floxed). Genes were considered differentially expressed at a fold change (log2): ≥1.5 or ≤−1.5; P < 0.05. (B) Representative quantitative real-time RT-PCR (qRT-PCR) for the indicated targets in sorted LSKs. Values are standardized to expression of β-actin and are presented as fold induction, relative to expression in control LSK cells (set as 1). Value for *Cebpa* from *Ctnnb1*(Ex3)Δ/+ LSK is 0.016 ± 0.015. Data are representative of three experiments. Error bars indicate SD, *n* = 3. (C) Immunoblot analysis of Irf8 protein in lineage depleted (Lin−) BM cells. Total protein extracts of poly(I:C)-treated controls and *Ctnnb1*(Ex3)Δ/+ mice (*n* = 3) were analyzed using an antibody against mouse Irf8. Tubulin staining was used as loading control. (D) GSEA comparison of the *Ctnnb1*(Ex3)Δ/+ against control LSKs for enrichment of *Irf8*-regulated genes. NES and p-values are indicated. (E) Identification of the Tcf/Lef1 binding sequences in the *Irf8* promoter (Shtutman et al., 1999). A schematic representation of the *Irf8* promoter structure with sequences of three putative TBEs. (F) Luciferase reporter assay showing the effect of β-catenin on the *Irf8* promoter activity. Four *Irf8* promoter fragments, F1/F0 (−1710 to +33), F2/F0 (−1582 to +33), F3/F0 (−1318 to +33), and F2*/F0 with mutation in TBE2 (−1582 to +33, mutation indicated by asterisks), were PCR amplified from mouse genomic DNA and cloned into the pGL3 basic Luciferase vector. 293T cells were cotransfected with respective reporter constructs, with or without chimeric β-catenin/Lef1 expression plasmid and were analyzed after 48h. β-Galactosidase construct was cotransfected to each sample to normalize transfection efficiency. The ratio of reporter luciferase activity to control β-galactosidase activity is indicated. Data are representative of three experiments. Error bars indicate SD, *n* = 3. (G) EMSA showing that Lef1 binds to *Irf8*

In addition, our experiments revealed *Irf8* as a novel Wnt/β-catenin–activated target gene that, in response to Wnt/β-catenin signaling, limits myeloid differentiation and proliferation.

Wnt/β-catenin signaling is essential for *Irf8*-deficient CML

Irf8 deficiency endows myeloid progenitors with proliferative and survival advantages (Gabriele et al., 1999; Scheller et al., 1999). Furthermore, a recent study showed that *Irf8* might modulate the stability of β-catenin (Huang et al., 2010), raising the possibility that both pathways are mechanistically connected. To examine the functional significance of β-catenin in the development of *Irf8*$^{-/-}$ CML-like disease, we conditionally deleted β-catenin in *Irf8*$^{-/-}$ BM cells by combining *Irf8*-null alleles with MxCre-inducible β-catenin floxed alleles (Huelsken et al., 2001; Jeannet et al., 2008). BM cells from inducible *Irf8*$^{-/-}$MxCre$^+$*Ctnnb1*$^{fl/fl}$ (denoted as DKO) and noninducible *Irf8*$^{-/-}$MxCre$^-$*Ctnnb1*$^{fl/fl}$ (denoted as *Irf8*$^{-/-}$) mice were used for reconstitution of lethally irradiated congenic WT recipients (B6.SJL, Ly5.1) and β-catenin deletion upon administration of poly(I:C) was induced after stable engraftment and monitored by PCR (Fig. 2, A–C). Although deletion of β-catenin did not affect hematopoiesis in the WT background (Jeannet et al., 2008), myeloproliferation was strongly affected in the *Irf8*-deficient background. Analysis of recipients bearing DKO cells revealed reduction of peripheral white blood cell (WBC) and of spleen weight within 30 d after β-catenin deletion (Fig. 2, D and E). The number of DKO LSK cells in BM and in spleen was profoundly reduced due to impaired frequencies of LT-HSCs (LSK, Flt3$^-$CD150$^+$) and ST-HSCs (LSK, Flt3$^-$CD150$^-$) compared with the recipients with single *Irf8*$^{-/-}$ (Fig. 2 F). The absolute number and frequency of DKO GMPs was strongly reduced as well (P < 0.0001), whereas both common myeloid progenitors (CMPs) and megakaryocyte/erythrocyte progenitors (MEPs) remained unchanged (Fig. 2 G). Loss of β-catenin did not alter the differentiation potential or apoptosis of DKO LSK and myeloid progenitors (Lin$^-$Sca-1$^-$c-kit$^+$); however, the number of mature granulocytes was reduced, whereas erythroid and lymphoid cell numbers were similar to WT (not

depicted). Altogether, the changes in BM and in extramedullary organs were characterized by depletion of the immature stem and GMP-progenitor compartments and a profound reduction of the CML-like phenotype in *Irf8*-deficient cells upon β-catenin deletion.
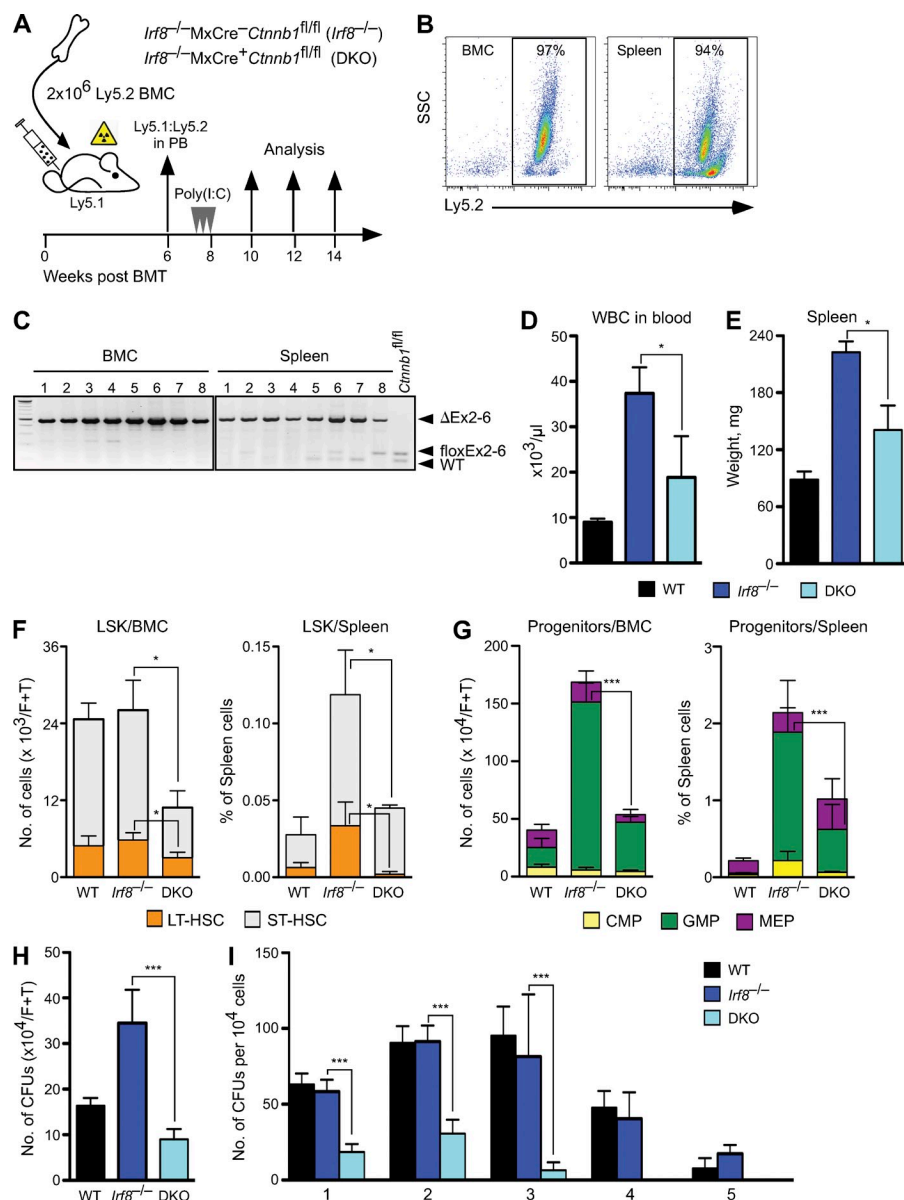
Because β-catenin may regulate self-renewal (Reya et al., 2003), we examined whether loss of β-catenin alters the clonogenic potential and self-renewal capacity of *Irf8*$^{-/-}$ cells. When BM and/or spleen cells were plated in semisolid medium, the number of colonies was strongly reduced in the DKO (Fig. 2 H, and not depicted for spleen). Serial replating showed that WT and *Irf8*$^{-/-}$ cells could be passaged more than four times, whereas DKO cells failed to replate beyond the second passage (Fig. 2 I). Decreased serial replating potential and colony formation suggested that deletion of β-catenin restricted self-renewal of *Irf8*-deficient cells. Thus, unlike in *Irf8*-proficient cells, where β-catenin was dispensable for colony formation (Cobas et al., 2004; Jeannet et al., 2008; Koch et al., 2008), self-renewal and proliferation of preleukemic *Irf8*$^{-/-}$ cells depend on β-catenin.

Enhanced β-catenin activity drives *Irf8*$^{-/-}$ CML into blast crisis

A chronic CML-like phase develops in *Irf8*$^{-/-}$ mice very rapidly with 100% penetrance, but transition to blast crisis occurs rarely and only after long latency (not depicted; Holtschke et al., 1996). This points to additional genetic lesions, which are required for transition into the acute BP. Considering the observation that the amplitude of Wnt/β-catenin signaling may control preleukemic and leukemic stem cells (Lane et al., 2011), we examined whether activation of β-catenin could promote *Irf8*-deficient leukemia. *Irf8*$^{-/-}$ mice were crossed to MxCre$^+$*Ctnnb1*$^{(Ex3)fl/+}$ or to control MxCre$^-$*Ctnnb1*$^{(Ex3)fl/+}$ mice and their BM was transplanted into lethally irradiated congenic WT recipients (B6.SJL, Ly5.1). After successful reconstitution (85–99% of donor cells), recipients were treated with poly(I:C) to activate Wnt/β-catenin signaling.

Recipients containing *Irf8*$^{-/-}$*Ctnnb1*$^{(Ex3)Δ/+}$ mutant cells showed extended survival, as compared with recipients

---

Tcf/Lef1 sites. 293T cells were transfected with pCG-Lef1-HA or with a mock control. Nuclear extracts were incubated with an α^{32}-P–labeled probe containing an *Irf8* Tcf/Lef1 site alone or with the addition of unlabeled competitors: the same WT *Irf8* Tcf construct, or a mutated *Irf8* Tcf construct (CTTTGAT to CTTTGGC), or a control oligonucleotide for a known human Cyclin D1 Tcf site without and with mutation (CTTTGAT to CTTTGGC). For supershift experiments, 2 μl anti-HA antibody (Santa Cruz Biotechnology, Inc.) was added. Incubation of nuclear extracts with an α^{32}-P–labeled probe containing a mutated *Irf8* Tcf site (CTTTGAT to CTTTGGC) did not show specific binding or supershift. Positions of the Lef1 protein (Lef1), the supershift band (ss), and free probe are indicated. (H) Overexpression of *Irf8* blocks myeloid differentiation in vivo. Lin$^-$ WT BM cells were transduced with a 4-OHT–inducible *Irf8*-ER^{T2} or an empty control (ER^{T2}) vectors. Cells were transplanted in lethally irradiated WT mice (n = 5 for each transduction). Relative changes of GFP-positive myeloid (CD11b$^+$) and B-lymphoid (B220$^+$) in peripheral blood plotted as percentages against time (weeks) after 4-OHT–mediated induction. Data are representative of two experiments. Error bars indicate SD, n = 5. (I) CFU assay in methylcellulose (M3434) from GFP$^+$-sorted BM cells retroviral infected with control (MSCV-IRES-eGFP), *Irf8*, and the stabilized form of β-catenin (β-cat*; β-catenin MSCV-β-catΔGSK-IRES-eGFP). Numbers of colonies per 10^4 cells plated are shown. Colonies were classified into granulocyte-macrophage (CFU-GM), macrophage (CFU-M), and granulocyte (CFU-G). Data represent the mean ± SD from three independent samples. (J) *Irf8* deficiency rescues myelopoiesis after activation of β-catenin in vitro. Lin$^-$ BM cells from WT and *Irf8*$^{-/-}$ mice were transduced with stabilized form of β-catenin (β-cat*) or control empty retrovirus; GFP$^+$ cells were sorted and assessed for myeloid differentiation in CFU assay. Colonies were counted and colony type confirmed by morphological analysis (May-Grunwald-Giemsa staining). Mean values ± SD from one representative experiment performed in triplicate out of three independent experiments is displayed. Statistics: (B, F, and H) Student´s *t* test. *, P < 0.05; **, P < 0.001; ***, P < 0.0001.

Figure 2. *Irf8*-deficient CML requires β-catenin. (A) Schematic representation of the experimental procedures and genotypes used for BM cell transplantation into lethally irradiated recipients. WT, noninducible *Irf8*$^{-/-}$ MxCre$^-$*Ctnnb1*$^{fl/fl}$ (*Irf8*$^{-/-}$) and inducible double knockout mutant *Irf8*$^{-/-}$MxCre$^+$*Ctnnb1*$^{fl/fl}$ (DKO) BM cells (Ly5.2$^+$) were injected into lethally irradiated congenic B6.SJL (Ly5.1$^+$) hosts, *n* = 10 recipients for each genotype. After 6 wk, reconstituted recipients were treated with poly(I:C) three times every 2nd d. (B) BM and spleen engraftment of donor-derived cells (Ly5.2$^+$) in B6.SJL (Ly5.1$^+$) recipients 30 d after poly(I:C) treatment. (C) Whole BM and spleen from B6.SJL recipients genotyped for deletion of β-catenin. (D and E) β-Catenin deletion reduces *Irf8*$^{-/-}$ myeloproliferative disease. Three to four mice per genotype were used to determine number of WBC in peripheral blood (D) and the mean weights of spleen from recipient mice ± SD transplanted with WT, *Irf8*$^{-/-}$, or DKO cells 30 dpi with poly(I:C) (E). (F and G) β-Catenin deletion results in reduction of stem and progenitor cells in recipients bearing DKO cells. Data represent mean ± SD from one experiment 30 d after the last p(I:C) injection, three to four mice per genotype were used. (F) Displayed are absolute number of LSKs in BM (left) and frequency of LSK in spleen (right). LSK compartment was subfractioned into LT-HSC and ST-HSC based on the surface expression of CD150 and Flt3 by FACS. (G) Absolute number of myeloid progenitors, separated as CMP, GMP, and MEP in BM (left) and their frequency in spleen (right) by FACS is shown. (H) Number of colonies derived from BM cells of recipients (described in D and E) tested in CFU assay. CFU per 2 × 10^4 cells were counted 7 d after cultivation and absolute numbers per femur and tibia are shown. Error bars indicate SD of mean number of colonies from t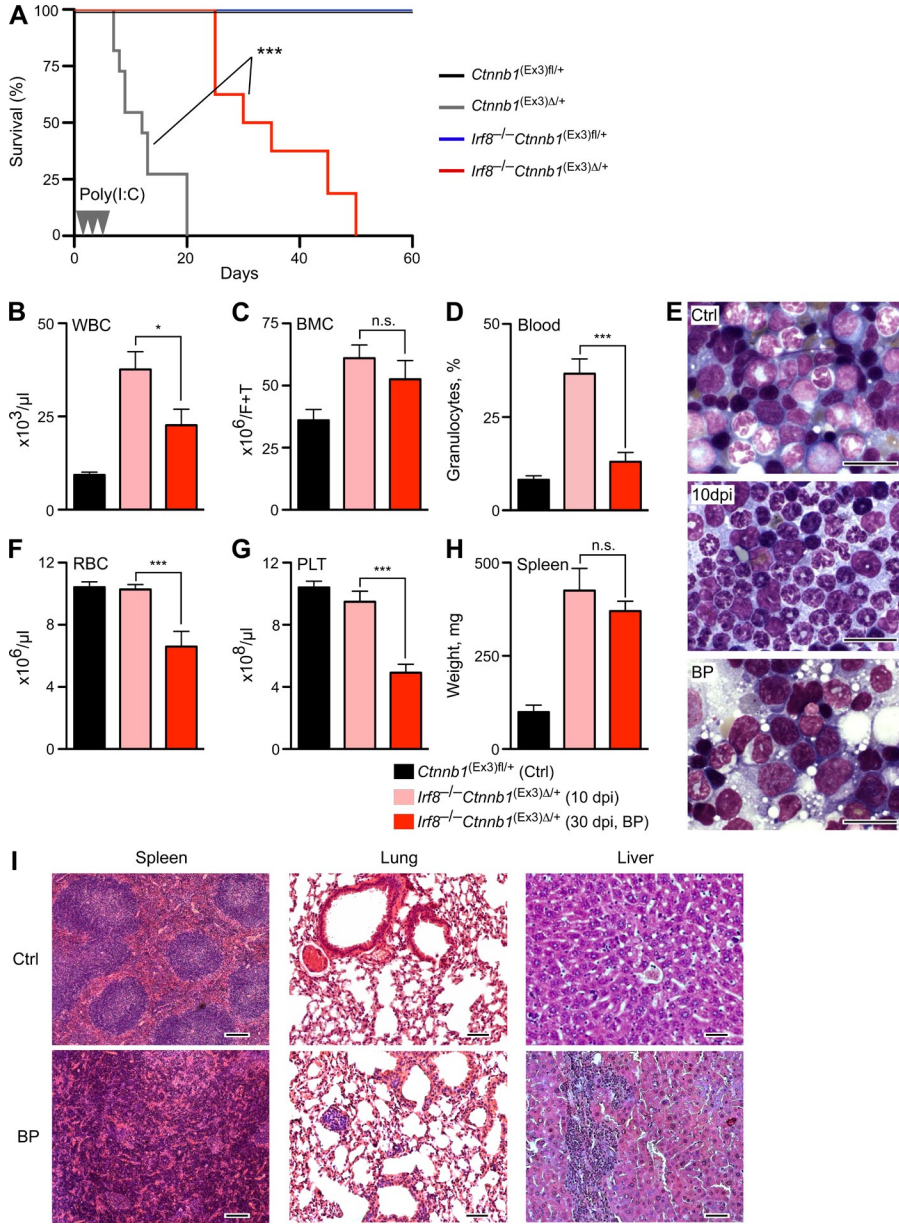riplicate cultures of each mouse (*n* = 3 in each group). (I) Serial replating assay of 1 × 10^4 BM cells in methylcellulose medium from indicated genotypes. Colonies were counted after 5 d. The same number of cells was used for replating (five rounds). Error bars indicate SD of mean number of colonies from triplicate cultures of each mouse (*n* = 3 in each group). Results are representative of two determinations performed with BM and spleen cells. Statistics: (D–I) Student's *t* test. *, P < 0.05; ***, P < 0.0001.

receiving single mutant *Ctnnb1*$^{(Ex3)\Delta/+}$ cells (Fig. 3 A), probably due to the apoptosis resistance of *Irf8*-deficient cells (Gabriele et al., 1999; Scheller et al., 1999). Deletion of a single *Irf8* allele (*Irf8*$^{+/-}$ *Ctnnb1*$^{(Ex3)\Delta/+}$) failed to increase survival, suggesting that complete loss of *Irf8* was required to overcome the lethality after β-catenin stabilization (unpublished data). 10 d post injection (dpi) with poly(I:C), recipients bearing *Irf8*$^{-/-}$ *Ctnnb1*$^{(Ex3)\Delta/+}$ cells displayed increased numbers of WBC and BM cells, with predominance of mature granulocytes (Fig. 3, B–D [pink bars, 10 dpi] and E [middle]) representing initial chronic CML-like disease, similar to *Irf8*$^{-/-}$ mice. However, at 20 dpi after β-catenin activation, the initially prevalent

neutrophilia was replaced by immature myeloid blasts (Fig. 3 E, bottom), and mice became anemic, moribund, or died. The number of differentiated WBCs in peripheral blood and BM cellularity was reduced (Fig. 3, B–D, red bars) and accompanied by development of a severe diffuse BM fibrosis, which in human is known to correlate with an unfavorable course of CML disease (Buesche et al., 2007). The number of red cells and platelets dropped (Fig. 3, F and G), and the spleen was enlarged, showing hyperplasia of red pulp and increased myelo-erythropoiesis with undifferentiated features (Fig. 3, H and I). Histological inspection revealed massive hematopoietic infiltrates in liver and pulmonary tissue (Fig. 3 I).

Figure 3. Activation of β–catenin accelerates CML–like disease of *Irf8*^{−/−} mice into blast crisis. (A) Kaplan-Meier survival curves of B6.SJL recipients transplanted with control MxCre[−]*Ctnnb1*[(Ex3)fl/+] (denoted as *Ctnnb1*[(Ex3)fl/+], n = 18), MxCre[+]*Ctnnb1*[(Ex3)Δ/+] (denoted as *Ctnnb1*[(Ex3)Δ/+], n = 20), *Irf8*^{−/−}MxCre[−]*Ctnnb1*[(Ex3)fl/+] (denoted as *Irf8*^{−/−} *Ctnnb1*[(Ex3)fl/+], n = 16), and *Irf8*^{−/−}MxCre[+] *Ctnnb1*[(Ex3)fl/+] (denoted as *Irf8*^{−/−}*Ctnnb1*[(Ex3)Δ/+], n = 20) are shown, and poly(I:C) injections are indicated as arrowheads. Log-rank (Mantel-Cox) test. ***, P < 0.0001. (B–H) Comparison of hematopoietic parameters during progression of CML-like disease from initial phase (10 dpi with poly(I:C), pink) to BP (30 dpi, red) versus *Irf8*^{+/+}MxCre[−]*Ctnnb1*[(Ex3)fl/+] (Ctrl). (B) Absolute number of WBCs in peripheral blood (×10^{6}/ml). (C) BM cells (BMC, ×10[6] cells/femur+tibia). (D) Percentage of granulocytes in peripheral blood. (E) A representative May-Grunwald-Giemsa staining of BM smears from recipients bearing control and double mutated *Irf8*^{−/−} *Ctnnb1*[(Ex3)Δ/+] cells after 10 dpi and in BP (30 dpi) are shown. Bars, 20 µm. (F) RBC (10[6]/µl) counts. (G) Platelet counts (PLT, 10[6]/µl). (H) Weights of the spleens (in milligrams) are shown. Results are displayed as mean values ± SEM from six to eight mice in each group. Statistics: (B–H) Student's t test. n.s., not significant; *, P < 0.05; ***, P < 0.0001. (I) Representative histology (H&E stain) of CML-like BP disease in spleen, liver, and lung from recipients bearing *Irf8*^{−/−}*Ctnnb1*[(Ex3)Δ/+] versus control (Ctrl) cells. Bars: (spleen) 200 µm; (lung) 100 µm; (liver) 50 µm.

To further examine how activated β-catenin drives disease progression, we performed immunophenotyping in single *Irf8*^{−/−} cells and *Irf8*^{−/−}*Ctnnb1*[(Ex3)Δ/+] cells. The frequency and absolute number of phenotypic HSCs (LSKs compartment) was reduced in the BP compared with the CP-like phase of disease (Fig. 4, A and B, top). Analysis of the myeloid progenitor compartment indicated a severe reduction in the number of CMPs and MEPs during disease progression (Fig. 4 A, bottom), whereas the number of GMPs remains increased, in comparison with control mice (Fig. 4, A and B, bottom). Granulocytic maturation stages were further examined to assess the differentiation block of leukemic cells. During the BP, recipients bearing *Irf8*^{−/−}*Ctnnb1*[(Ex3)Δ/+] cells displayed more promyelocytes (2.1 vs. 0.8%) and a strong reduction of mature granulocytes (0.06 vs. 16%), reflecting a

block of granulocytic differentiation (Fig. 4, C and D). Collectively, these results showed that conditional activation of β-catenin shifts the initial CP of the *Irf8*^{−/−} CML-like disease into a fatal BP.

Next, we analyzed the cellular distribution of β-catenin during disease progression. Elevated amounts of β-catenin protein were found in the nuclear fraction of single *Irf8*^{−/−} Lin^{−} BM cells, which correlated with activated Wnt/β-catenin signaling and was even more increased in double mutated *Irf8*^{−/−}*Ctnnb1*[(Ex3)Δ/+] cell nuclei (Fig. 4 E). This indicates that the level of β-catenin activation could be responsible for disease progression and that enhanced β-catenin activation in Irf8^{−/−}*Ctnnb1*[(Ex3)Δ/+] cells is a prerequisite for shifting the initial CP of the *Irf8*^{−/−} CML-like disease into a fatal blast crisis with accumulation of GMP-like blasts.
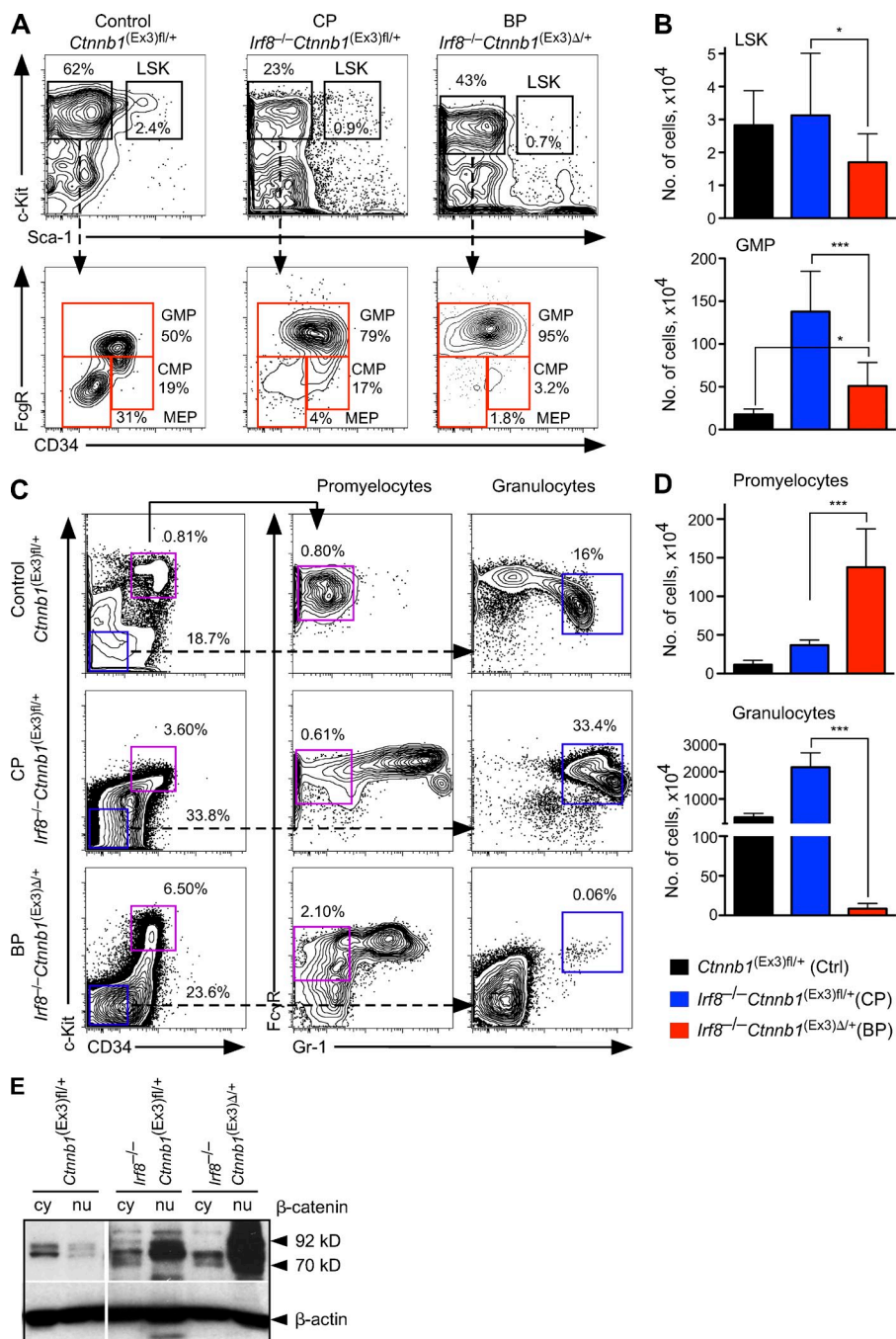
Figure 4. Immunophenotyping of HSCs and myeloid progenitors from leukemic mice. (A) Reorganization of the immature BM compartments in transplanted mice in different stages of disease progression. Representative FACS profiles for LSKs (top), represented as percentage of lineage-negative LSK BM fraction and myeloid progenitors (bottom), separated by FcγR versus CD34 staining as GMPs, CMPs, and MEPs from recipients transplanted with control $Ctnnb1^{(Ex3)fl/+}$, $Irf8^{-/-}$ (CP), and $Irf8^{-/-}$ $Ctnnb1^{(Ex3)\Delta/+}$. (B) Absolute numbers of LSKs (top) and GMPs (bottom) in BM per femur and tibia. (C) Expansion of promyelocytes expressing activated β-catenin in the BP phase. Lin−, Sca-1–negative BM cells in control, CP, or BP were gated into c-Kit+ CD34+ and c-Kit−CD34− fractions (left). Promyelocytes were gated based on c-Kit+ CD34+Gr-1+ immunophenotype (middle) and mature granulocytes were gated based on c-Kit− CD34−Gr-1+ immunophenotype (right). Frequencies are represented as percentage among all live cells. (D) Absolute numbers of promyelocytes (top) and granulocytes (bottom) in BM per femur and tibia. Data in B and D are mean ± SD for 8–10 mice of each genotype. Statistics: (B and D) Student's t test. *, P < 0.05; ***, P < 0.0001. (E) Immunoblot analysis of β-catenin protein localization in stem and progenitor cells enriched Lin− BM fractions. The cytoplasmic (cy) and nuclear (nu) fractions were analyzed using an anti–β-catenin antibody for the poly(I:C)-treated control $Ctnnb1^{(Ex3)fl/+}$, $Irf8^{-/-}$ $Ctnnb1^{(Ex3)fl/+}$ (n = 3), and double-mutated $Irf8^{-/-}$ $Ctnnb1^{(Ex3)\Delta/+}$ (n = 4) cells. β-Actin staining served as loading control.

Decreased expression of *Irf8* and increased activation of β-catenin are clinically relevant (Schmidt et al., 2001; Jamieson et al., 2004). We referred to published datasets to assess frequency of compound lesions (Radich et al., 2006). We observed a striking down-regulation of *IRF8* expression during CML progression in a large cohort of accelerated and BP of CML samples, as compared with the CP (P < 0.05; Fig. 5 A). A significant proportion of these patients also showed accompanying up-regulation of Wnt/β-catenin target genes (Fig. 5 B, mean P < 0.05), whereas BP patients with normal- or up-regulated levels of *IRF8* showed no significant mean p-value

(Fig. 5 C, mean P = 0.8666). These results corroborated the presumption of simultaneous deregulation of *IRF8* and Wnt/β-catenin in human CML progression.

Activation of β-catenin determines the extent of gene regulation in leukemic GMPs from chronic to BP transition

Similar to the results shown here, expansion of progenitors and reduction of HSC was found in the BM from patients with blast-crisis CML (Jamieson et al., 2004). We therefore analyzed gene expression from sorted murine LSK and GMP populations after development of clinically evident blast crisis
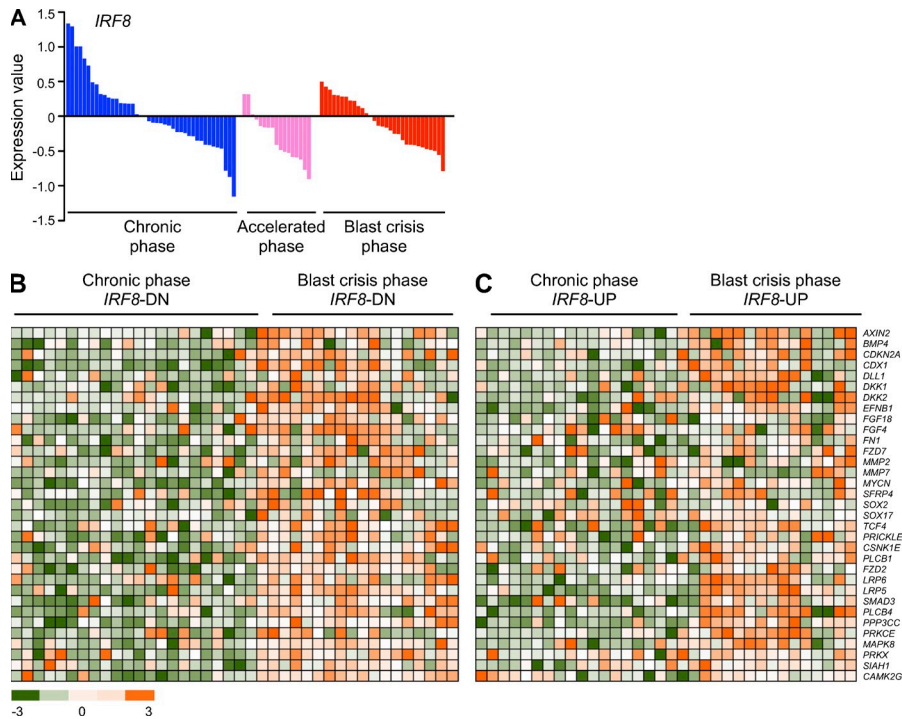
Figure 5. Gene expression profile in BM or PB from chronic and BP CML patients. (A) Expression of *IRF8* (P < 0.05) in BM or PB from CP (blue), accelerated phase (pink), and BP (red) CML patients is displayed in linear scale. Data were analyzed using R/Bioconductor, and moderated *t*-statistics using the limma package. (B and C) The samples were separated into *IRF8*-down (*IRF8*-DN, B) and *IRF8*-up-regulated (*IRF8*-UP, C) subgroups. Heatmaps show representative Wnt target genes. Microarray data were taken from the Gene Expression Omnibus under accession no. GSE4170.

in recipients bearing $Irf8^{-/-}Ctnnb1^{(Ex3)\Delta/+}$ cells and compared them with controls ($Ctnnb1^{(Ex3)fl/+}$). The numbers of differentially expressed genes in leukemic $Irf8^{-/-}Ctnnb1^{(Ex3)\Delta/+}$ GMPs were higher than in LSKs (Fig. 6 A), indicating that major differences occur at the level of GMP rather than at the LSK stage. Compared with LSKs, gene profiling of $Irf8^{-/-}Ctnnb1^{(Ex3)\Delta/+}$ GMPs showed strong enrichment of a leukemic self-renewal–associated signature, as reported for an AML-AF9–transformed functionally defined L-GMP population (Krivtsov et al., 2006; Fig. 6 B) and for up-regulated genes derived from human CML patients (Diaz-Blanco et al., 2007; Fig. 6 C). Furthermore, reduction of LSK and accumulation of GMP in the BP was consistent with an increased proapoptosis-associated gene set seen in $Irf8^{-/-}Ctnnb1^{(Ex3)\Delta/+}$ LSK in contrast to the $Irf8^{-/-}Ctnnb1^{(Ex3)\Delta/+}$ GMPs gene profiles (Fig. 6 D).

Interestingly, applying established myeloid (GM)- and megakaryocyte/erythroid (MkE)-specific gene sets (Månsson et al., 2007), the GMP profiles of $Irf8^{-/-}Ctnnb1^{(Ex3)\Delta/+}$ cells showed enrichment for GM signatures and depletion for MkE signatures (Fig. 6 E), whereas single mutated $Ctnnb1^{(Ex3)\Delta/+}$ GMP profiles displayed inverse gene set enrichment (Fig. 1 A), reflecting defects in lineage commitment. These results suggest that *Irf8* is involved in the suppression of myeloid-specific genes by activated β-catenin.

To examine how enhanced β-catenin signaling advances $Irf8^{-/-}$ CML-like disease into BP, we compared global gene expression in GMP samples from three phenotypes: control, single $Irf8^{-/-}$ (denoted as CP), and double mutated $Irf8^{-/-}Ctnnb1^{(Ex3)\Delta/+}$ (denoted as BP). Unsupervised analysis demonstrated that $Irf8^{-/-}Ctnnb1^{(Ex3)\Delta/+}$ GMPs from BP have an

expression profile that is different from the control but is similar to the $Irf8^{-/-}$ GMPs (unpublished data). Hierarchical clustering using the Ward algorithm and Pearson's correlation identified a large group of genes with similar expression in both GMPs from CP and BP, but significantly enhanced deregulation in the $Irf8^{-/-}Ctnnb1^{(Ex3)\Delta/+}$ GMP from BP, establishing a progression-specific signature (PSS; Fig. 6 F; available online under accession no. GSE49054). All transcripts deregulated in PSS from $Irf8^{-/-}Ctnnb1^{(Ex3)\Delta/+}$ GMPs showed a significantly restricted expression level in the CP compared with the acute BP (Fig. 6 G). These results suggest that the biological differences between chronic and BPs of myeloid leukemia are likely mediated by quantitative alterations in gene expression and that activated β-catenin controls the extent of gene regulation.

Classification of PSS genes according to their functional annotation (GO/KEGG) revealed up-regulation of genes that belong to metabolic pathways, including lipid metabolism and glycolysis (Fig. 6 H). Moreover, progression was associated with up-regulation of MAPK, insulin, and VEGF signaling pathway genes, in addition to cytoskeletal and adhesion molecule alterations. Remarkably, ABC transporter genes, including *Abcb10*, *Abcc2*, and *Abcc5*, which are implicated in the development of drug resistance in human CML, were highly up-regulated, suggesting involvement of Wnt/β-catenin signaling in the regulation of ABC-transporter gene transcription. Compared with the CP, the β-arrestin2 (*Arrb2*) and *Bcl6* genes were up-regulated (accession no. GSE49054), both of which have recently been suggested as critical for LIC survival and progression of BCR-ABL–transformed CML in humans and in a mouse model (Hurtz et al., 2011; Fereshteh et al., 2012).
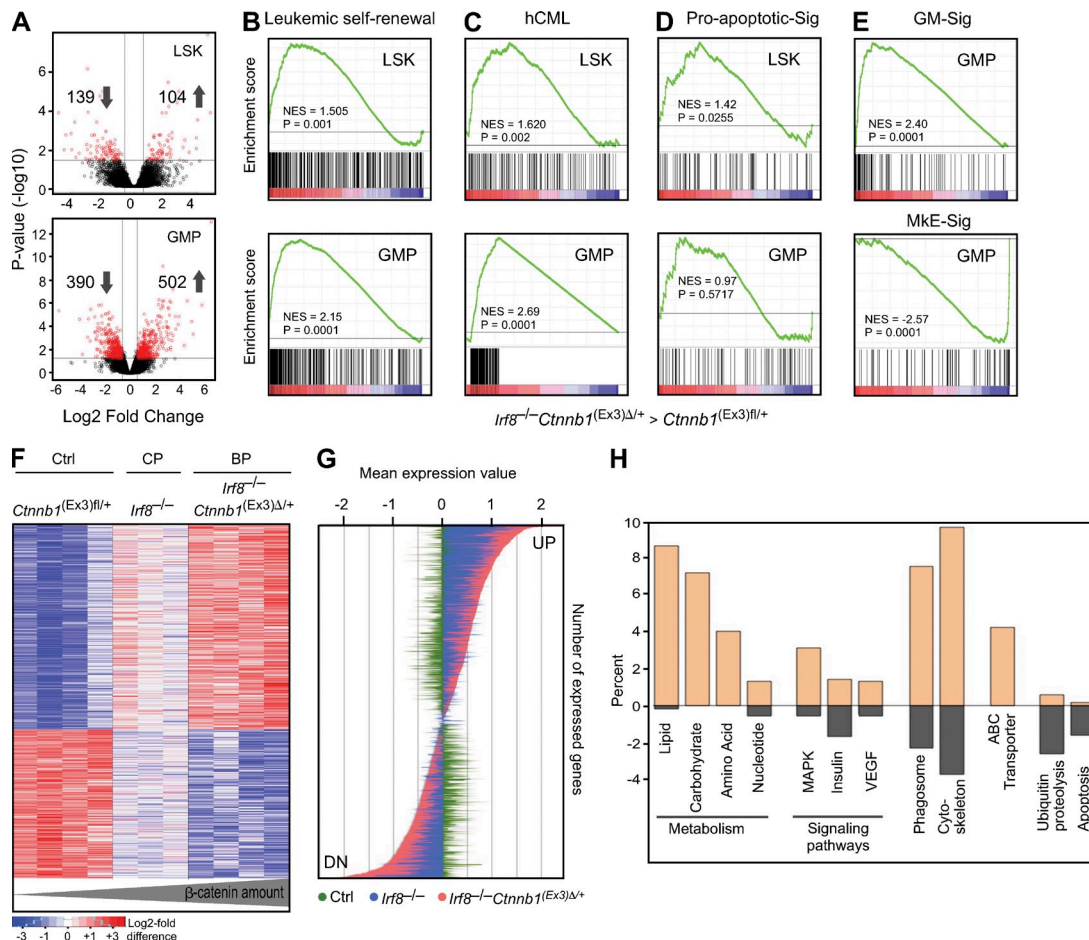
Figure 6. Gene expression profile of leukemic LSKs and GMPs. (A) Comparison of significantly differently expressed genes between control *Ctnnb1*[(Ex3)fl/+] and *Irf8*^{−/−}*Ctnnb1*[(Ex3)Δ/+] cells from sorted LSK (top) and GMP (bottom) populations is shown in Volcano plots. The negative log10-transformed p-values are plotted against log2 fold change. Red dots represent significant differentially expressed probe sets. (B–E) Comparison by GSEA between LSKs (top) and GMPs (bottom) from *Irf8*^{−/−}*Ctnnb1*[(Ex3)Δ/+]. Each population was compared individually to LSK and GMPs from control *Ctnnb1*[(Ex3)fl/+] profiles. Plots show enrichment/depletion of leukemic self-renewal associated genes derived from MLL-AF9-transduced L-GMPs (B) and up-regulated gene set from human CML patients (165 genes in enrichments core; C) and genes involved in proapoptotic signature (D; Reactome). (E) GSEA plots from *Irf8*^{−/−}*Ctnnb1*[(Ex3)Δ/+] GMPs compared with control *Ctnnb1*[(Ex3)fl/+] GMPs showing enrichment/depletion of granulocytic/monocytic- (GM-Sig, top) and mega-karyocytic/erythroid (MkE-Sig, bottom)-associated gene expression set. The NES and p-values are indicated on each plot. (F) Heatmap of significantly deregulated genes in GMPs from BP and CP compared with control establish a PSS; Pearson's correlation coefficient and Ward's method were used. (G) Expression values of up- and down-regulated genes as depicted in PSS. BP (red, genes in *Irf8*^{−/−}*Ctnnb1*[(Ex3)Δ/+] GMPs) as compared with CP (blue, genes in *Irf8*^{−/−} GMPs) and control (green, genes in *Ctnnb1*[(Ex3)fl/+] GMPs). The y-axis represents different genes from the PSS; the x-axis depicts the median expression value for every gene, which were row-wise median centered. (H) Gene ontology classification of genes selectively expressed in PSS. The percentage of each functional category represents numbers of gene transcripts that were more abundant in PSS profile than in control GMPs (plus value, up-regulated; minus value, down-regulated genes).

Among the down-regulated genes, proapoptotic genes and genes involved in ubiquitin-mediated proteolysis (*Cul4b*, *Nedd4*, *Fbxw4*, *Ubfd1*, and *Rhobtb1*) were prominent and diminished ubiquitin-mediated proteolysis has previously been associated with β-catenin stabilization (Aberle et al., 1997). Collectively, our data suggest that stepwise enhancement of β-catenin drives *Irf8*-deficient CML into acute BP. These blasts display more primitive but deregulated stem cell features with enrichment of genes associated with leukemic self-renewal and drug resistance.

Enhanced leukemic potential of BCR–ABL–induced LICs and Imatinib resistance depends on cooperation between β-catenin activation and *Irf8* deficiency

The murine BCR–ABL–mediated CML model was used to validate the finding of combined β-catenin and *Irf8* lesions in human CML. Lin[−] BMC from control (WT) and double mutant *Irf8*^{−/−}MxCre[+]*Ctnnb1*[(Ex3)fl/+] mice were transduced with a retrovirus expressing the p210*BCR-ABL*-GFP gene (Li et al., 1999). Transformation efficiency was indistinguishable, but *Irf8*^{−/−}MxCre[+]*Ctnnb1*[(Ex3)fl/+] cells without β-catenin
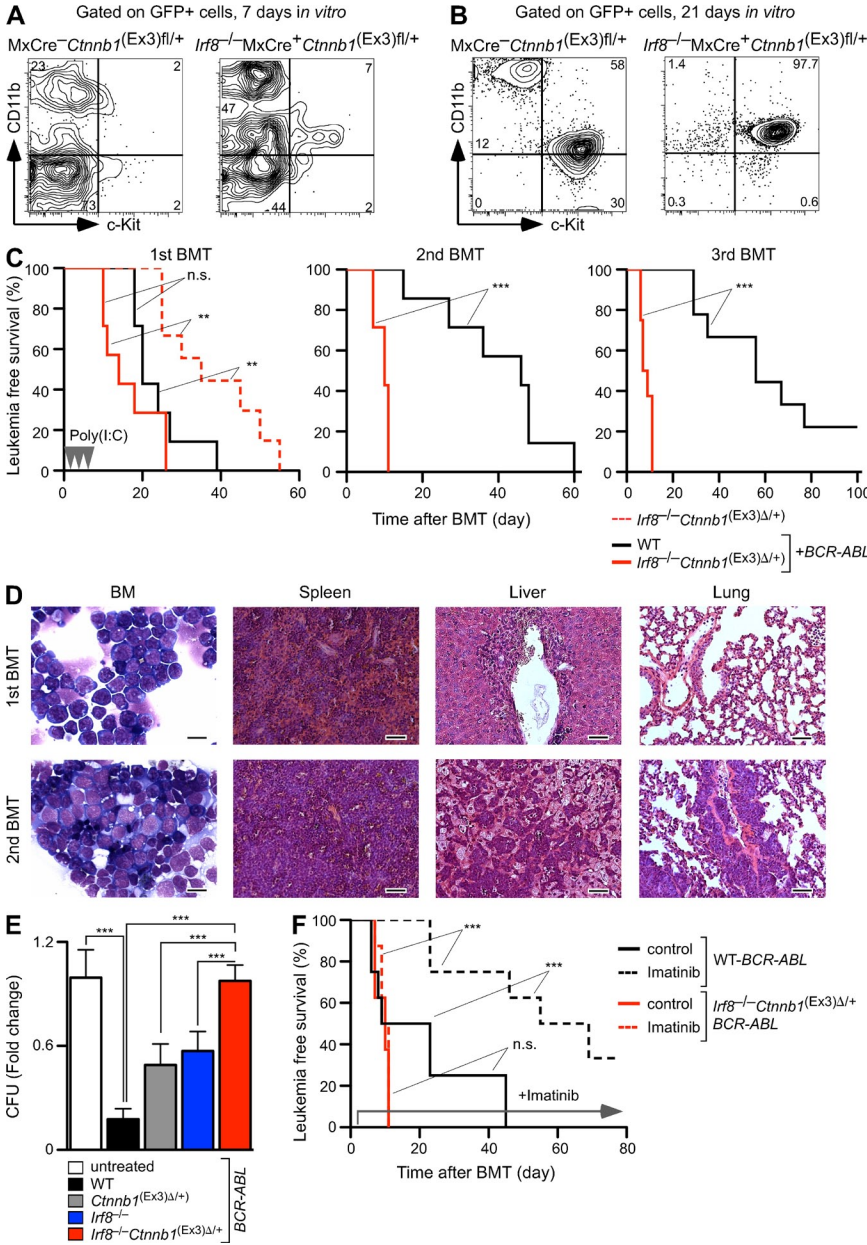
Figure 7. Enhanced leukemic potential of BCR-ABL–induced LICs and Imatinib resistance depends on cooperation between β-catenin activation and *Irf8* deficiency. (A and B) FACS analysis of GFP+ cells from BCR-ABL–transduced Lin− BMC at 7 (A) and 21 (B) d after expansion culture in vitro. GFP+ cells were sorted 48 h after retroviral infection and propagated in co-culture with OP9 stromal cells supplemented with SCF, Flt-3–ligand, and IL-7. (C) Kaplan-Meier survival curves of recipients from serial BMT assays. After injection of 5×10^3 sorted GFP+ cells plus 5×10^5 supporter cells, no significant difference in survival was evident in primary recipients (first BMT) bearing BCR-ABL–transfected control ($n = 10$) or $Irf8^{-/-} Ctnnb1^{(Ex3)\Delta/+}$ ($n = 10$) in comparison with non–BCR-ABL–transduced $Irf8^{-/-} Ctnnb1^{(Ex3)\Delta/+}$ cells. β-Catenin was activated by administration of poly(I:C) (injections shown as arrowheads). Transplantation of 5×10^3 sorted GFP+ cells from primary recipients and 5×10^5 supporter cells showed a significant increase in disease load in $Irf8^{-/-} Ctnnb1^{(Ex3)\Delta/+}$ secondary and tertiary recipient mice ($n = 10$ in each BMT), as compared with WT controls. Log-rank (Mantel-Cox) test. n.s., not significant; **, P < 0.001; ***, P < 0.0001. (D) Development of aggressive CML BP of disease during serial transplantation in recipients bearing $Irf8^{-/-} Ctnnb1^{(Ex3)\Delta/+}$ GFP+ cells. Blast cells in BM and organ infiltrations from first and second BMT mice are shown by May-Grunwald-Giemsa staining of BM smears and H&E stain of organs. Bars: (BM) 10 μm; (spleen, liver, and lung) 50 μm. (E and F) β-Catenin activation, *Irf8* deficiency, and Imatinib resistance in vitro and in vivo. (E) Effect of Imatinib treatment (5 μM) on LIC colony-forming ability in CFU assays. GFP+ cells from second BMT mice that were co-cultured on OP9 cells for 5 d in the absence or presence of 5 μM Imatinib. Values are standardized to CFU number from untreated cultures in each phenotype and are presented as fold change, relative to untreated cultures in control cells (set to 1; fold change of CFU number in response to Imatinib treatment in vitro). Error bars indicate SD of triplicates from one experiment. Two independent experiments with similar outcome were done. Student's *t* test. ***, P < 0.0001. (F) Imatinib administration prolongs the survival of CML-affected mice bearing control but not $Irf8^{-/-} Ctnnb1^{(Ex3)\Delta/+}$ LICs. At 7 d after second BMT (Fig. 7 C), recipients received Imatinib ($n = 10$ for each phenotype) or vehicle (control) for 70 d, and the percentage of survival was determined. Log-rank (Mantel-Cox) test. n.s., not significant; ***, P < 0.0001.

activation showed higher myeloid differentiation rate and accumulation of CD11b+c-Kit+ population in vitro (Fig. 7 A). After expansion in vitro, GFP+ cells from control cultures contained c-Kit+CD11b+ and c-Kit+CD11b− populations, whereas $Irf8^{-/-}MxCre^+Ctnnb1^{(Ex3)fl/+}$ cultures consisted mainly of a c-Kit+CD11b+ population (Fig. 7 B). To determine the leukemia-initiating potential of BCR-ABL–transformed cells (LICs) in vivo, GFP+c-Kit+CD11b+ cells (that also contained a GMP fraction) were sorted and transplanted into syngeneic recipients along with freshly isolated WT BM cells (first BM

transplantation [BMT]). The control recipient group, containing WT-BCR-ABL–transformed LICs (WT-LICs), succumbed to BCR-ABL–induced CML development with increased granulopoiesis and splenomegaly within 4 wk after transplantation (Fig. 7 C). In contrast, recipients bearing BCR-ABL–expressing $Irf8^{-/-} Ctnnb1^{(Ex3)\Delta/+}$ cells ($Irf8^{-/-} Ctnnb1^{(Ex3)\Delta/+}$-LIC) developed an aggressive acute BP shortly after β-catenin activation (Fig. 7 C). Importantly, the disease latency of $Irf8^{-/-} Ctnnb1^{(Ex3)\Delta/+}$ transplanted mice was significantly (P = 0.0004) shorter in the presence of BCR-ABL
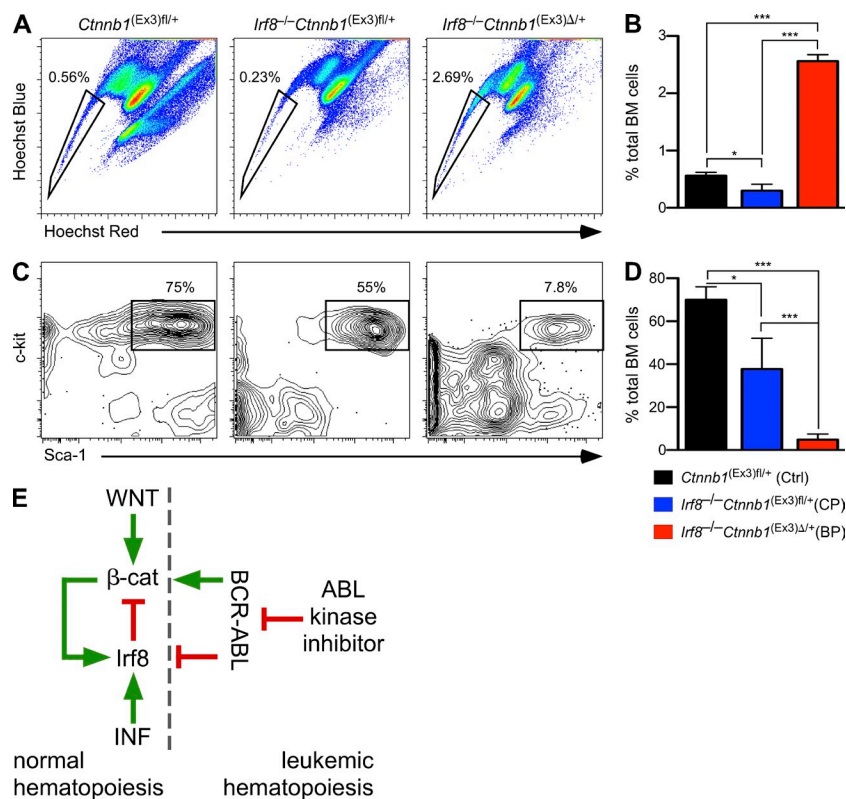
Figure 8. Enrichment of SP cells in *Irf8⁻/⁻ Ctnnb1*(Ex3)Δ/+ BM and conclusive model. (A–D) Hoechst 33342 profile and the immunophenotyping of SP cells shows. Data are mean values ± SD for three to four mice of each genotype. (A) Representative FACS analysis of control, *Irf8⁻/⁻*, and double-mutated *Irf8⁻/⁻ Ctnnb1*(Ex3)Δ/+ BM cells, which were stained with Hoechst 33342 dye to determine the Hoechst effluxing SP is shown. The SP region is indicated by a trapezoid on each panel. (B) Bar graph listing the frequency of SP cells among all single, viable, and nucleated cells shown in A. (C) Representative FACS profiles for LSKs represented as the percentage of LSK BM progenitors within gated SP cells. (D) Bar graph listing the frequency of LSKs within SP population shown in C. Statistics: (B and D) Student's *t* test. *, P < 0.05; ***, P < 0.0001. (E) Conclusive model summarizing the regulatory circuitry between Irf8, Wnt signaling, and BCR-ABL. Scheme outlining the crosstalk between Wnt and IFN signaling in normal hematopoiesis and interference by BCR-ABL signaling. In normal hematopoiesis, activation of β-catenin results in up-regulation of *Irf8* (green line), which in turn limits oncogenic β-catenin functions (red line). In leukemia BCR-ABL interferes with this cross talk by inhibiting *Irf8* and by activating β-catenin. Imatinib inhibits BCR-ABL and restores CML progression. Additional alterations at later stages of disease confer BCR-ABL–independent β-catenin activation and *Irf8* inhibition and thus cause Imatinib resistance.

than without it, indicating that addition of these genetic lesions accelerated BCR-ABL–induced leukemia progression. Absolute numbers of GFP⁺ *Irf8⁻/⁻ Ctnnb1*(Ex3)Δ/+-LICs in recipient peripheral blood were significantly higher than the absolute numbers of WT-LICs (96.85 ± 19.7 vs. 5.12 ± 0.6, ×10⁴/µl). Next, we performed serial transplantation of BCR-ABL⁺ WT- and *Irf8⁻/⁻ Ctnnb1*(Ex3)Δ/+-LICs from first BMT mice into a new set of recipients along with supporter BM cells. WT-LICs were still sufficient to induce CML in second BMT recipients but disease development and lethality declined in third BMT recipients (Fig. 7 C, middle and right). Conversely, *Irf8⁻/⁻ Ctnnb1*(Ex3)Δ/+-LICs gave rise to an accelerated course of disease through serial transplantations with rapid generation of undifferentiated blasts in BM, spleen, and peripheral organs (Fig. 7 D). Notably, we observed development of ALL or CML in second and third BMT recipients that had received either WT-LICs or *Irf8⁻/⁻ Ctnnb1*(Ex3)Δ/+-LICs (unpublished data), as reported (Li et al., 1999), suggesting that both LICs can generate malignancies in several lineages. Thus, results from serial transplantation assays demonstrated that cooperation between activated β-catenin signaling and *Irf8* deficiency maintains a long-term leukemia-initiating potential with increased self-renewal activity, whereas WT-LICs lose their leukemia-initiating potential, probably due to a reduction in LIC self-renewal activity.

Previous work by others suggested that either expression of *Irf8* or deletion of β-catenin correlated with increased Imatinib sensitivity of CML cells (Burchert et al., 2004; Heidel

et al., 2012). We therefore tested whether combined β-catenin activation and loss of *Irf8* synergistically interferes with Imatinib response to diminish BCR-ABL–induced CML. BCR-ABL–transformed LICs from different phenotypes were co-cultured with OP9 stromal cells in the presence of 5 µM Imatinib. WT-LICs were highly sensitive to Imatinib, as previously reported (Hurtz et al., 2011), and Imatinib treatment efficiently suppressed colony-forming potential in WT-BCR-ABL cells (Fig. 7 E). This response was reduced in cells either being *Irf8*-deficient or expressing stabilized β-catenin, but full resistance was not achieved. In contrast, *Irf8⁻/⁻ Ctnnb1*(Ex3)Δ/+ BCR-ABL–expressing cells showed complete Imatinib resistance, indicating that both mutations synergistically mediate drug resistance of BCR-ABL⁺ leukemia (Fig. 7 E). We validated these results in vivo by administration of Imatinib to second BMT mice bearing WT or *Irf8⁻/⁻ Ctnnb1*(Ex3)Δ/+ CML-LICs. Indeed, Imatinib treatment failed to inhibit disease development in recipients receiving *Irf8⁻/⁻ Ctnnb1*(Ex3)Δ/+-LICs and the animals developed BP and died, whereas WT-LIC recipients were rescued by Imatinib treatment (Fig. 7 F). Thus, synergistic up-regulation of *Irf8* and down-regulation of β-catenin could be essential for sensitization of CML-LICs to Imatinib treatment.

Gene expression profiling of *Irf8⁻/⁻ Ctnnb1*(Ex3)Δ/+ cells showed up-regulation of several ABC transporter genes (Fig. 6 H), which had been suggested to be involved in active TKI efflux and TKI resistance (Zhou et al., 2001; Jordanides et al., 2006; Deenik et al., 2010). We therefore examined the dye-excluding

side population (SP) of CML-LICs to explore enhanced efflux as a possible mechanism of Imatinib resistance. An increased SP was detected in $Irf8^{-/-}Ctnnb1^{(Ex3)\Delta/+}$, as compared with single $Irf8^{-/-}$ and WT Lin-depleted BM cells (Fig. 8, A and B). Further characterization revealed that WT contained a homogenous LSK-enriched SP, whereas the $Irf8^{-/-}Ctnnb1^{(Ex3)\Delta/+}$ SP was heterogeneous and contained more differentiated and fewer LSK cells (Fig. 8, C and D). These results suggest enhanced efflux as a mechanism of resistance to Imatinib therapy.

DISCUSSION

The clinical observation of *Irf8* deficiency and enhanced Wnt/β-catenin pathway activity predicts poor prognosis in the progression of myeloid leukemia (Schmidt et al., 2001; Jamieson et al., 2004). However, genetic evidence of functional interaction between both genetic lesions was missing. Using conditional gene targeting in mice, we show a direct cross-regulatory relationship between *Irf8* and canonical Wnt signaling in leukemia, as depicted in Fig. 8 E. Previously, we and others showed that activation of β-catenin in WT HSCs failed to induce leukemia (Kirstetter et al., 2006; Scheller et al., 2006). Here, we demonstrate that this failure is caused by a feedback loop between the Wnt/β-catenin signaling and the *Irf8* gene. Loss of *Irf8* led to preleukemic myeloproliferation, which required β-catenin. Increasing the dosage of activated β-catenin in *Irf8*-deficient cells advanced the chronic CML into an acute disease phase, providing genetic evidence that *Irf8* is a roadblock for β-catenin–induced leukemogenesis. Accordingly, β-catenin activation in combination with *Irf8* deficiency represent molecular events that increase the leukemic potential of BCR-ABL–transformed LICs, aggressiveness of CML progression, and rendered LICs resistant to Imatinib (Fig. 8 E).

The murine model described here recapitulates both phases of classical human CML: (1) an initial semi-stable CP that entails compromised *Irf8* expression and low-level nuclear β-catenin expression; and (2) a subsequent acute and fatal BP that entails strongly increased accumulation of nuclear β-catenin combined with loss of *Irf8*. How *Irf8* could reduce β-catenin nuclear accumulation is issue of further studies, although a possible explanation relates to altered proteasomal degradation. In $Irf8^{-/-}$ cells, transcripts encoding ubiquitin-mediated proteolysis pathway components including *Cul4b*, *Fbxw4*, *Ubfd1*, and *Rhobtb1*, are down-regulated. It has been shown that these gene products may be involved in β-catenin turnover (Aberle et al., 1997). Thus, different quantities of activated β-catenin drive the chronic and acute leukemogenic phases. Similarly, LICs in MLL-induced leukemia were demonstrated to express high levels of activated β-catenin, as compared with pre-LICs (Yeung et al., 2010). It has also been proposed that Wnt/β-catenin signaling regulates normal adult hematopoiesis in a dosage-dependent manner (Luis et al., 2011) and that the degree of activated β-catenin in a "just-right" signaling model, as proposed for allophycocyanin (APC), could be relevant for tumor formation in different tissues

(Fodde et al., 2001). Collectively, it appears that the amount of activated β-catenin in the nucleus determines the severity of the disease. Although because BP occurs relatively late after β-catenin stabilization, we cannot exclude that additional molecular changes are required for disease progression.

Self-renewing HSCs are maintained after conditional removal of β-catenin, γ-catenin, or both, whereas aberrantly activated Wnt/β-catenin signaling reactivates a self-renewal program of LICs in various hematopoietic disorders. We demonstrated that constitutive activation of β-catenin in WT HSCs results in down-regulation of self-renewal–associated genes and up-regulation of apoptotic genes (Fig. 1 A), in accordance with previous observations (Kim et al., 2000; Perry et al., 2011). Indeed, competitively transplanted cells with unrestricted β-catenin activation disappeared in recipients, indicating selective disadvantage of such hematopoietic progenitors that may be superseded only when cells become resistant to apoptosis (Reya et al., 2003; Perry et al., 2011). *Irf8*-mediated apoptosis and tumor suppression has been reported to occur in part by *Bcl2* down-regulation (Tamura et al., 2003; Burchert et al., 2004). Moreover, stabilized β-catenin was tolerated in myeloid cells that ectopically express *Bcl2* (Reya et al., 2003). We therefore examined whether *Bcl2* deregulation would suffice for acute leukemogenic conversion after Wnt/β-catenin signaling activation (constructing MxCre$^+$*Ctnnb1*$^{(Ex3)fl/+}$ and H2K-BCL-2 intercrosses. Although these results confirmed attenuated leukocytosis and expansion of the LSK compartment in *Bcl2* transgenic animals after stabilization of β-catenin (unpublished data), protection from apoptosis was not sufficient for myeloid leukemia development. Similarly, *Irf8* haploinsufficiency did not cooperate with antiapoptotic signals delivered by *Bcl2* to promote leukemia (Koenigsmann and Carstanjen, 2009).

In accordance with a previous study (Baba et al., 2005), β-catenin activation skews the lineage-priming gene pattern in WT HSCs and GMPs by suppression of myeloid and up-regulation of erythroid genes (Fig. 1 A). Although myeloerythroid transcriptional deregulation is often associated with leukemogenesis, it may thus be considered as a consequence, rather than the cause of malignancy (Jamieson et al., 2004; Rosenbauer and Tenen, 2007). Deregulation of myelo-erythroid lineage priming may be caused in part by enhanced *Irf8* expression that acts as a myeloid gene suppressor and therewith restricts the myeloid lineage commitment phase that is particularly vulnerable to leukemic conversion (Kirstetter et al., 2008; Zhang et al., 2009). Importantly, genetic ablation of *Irf8* restores the myeloid lineage capacity of GMPs, defeats apoptosis, and permits activated β-catenin to drive leukemogenesis.

The conditional induction of BP after β-catenin activation in *Irf8*-deficient mice permitted the direct comparison of gene profiles between the chronic and the acute leukemic phase. This revealed that progression of the disease is tightly connected to the magnitude of deregulation of a gene set (PSS) that is already present in the CP. Consistent with this notion is the fact that only a modest number of genes was previously found to be differentially expressed during progression

of human CML disease; 34 genes were associated with CML progression and malignancy of blasts, and 6 genes were proposed as diagnostic markers (Zheng et al., 2006; Oehler et al., 2009).

Gene expression profiling of the GMP-like population in BP revealed a signature shared with MLL-AF9–transformed AML (Krivtsov et al., 2006) and with up-regulated gene set from human CML patients (Diaz-Blanco et al., 2007). Notably, *Hoxa9*, *Meis1*, and *Mef2c* genes that are characteristic for MLL rearrangements and an HSC–associated self-renewal signature were down-regulated in GMPs from BP, indicating that transformation in the GMP compartment may also occur without deregulation of these genes, although their importance has been shown in human MLL-induced AML (Krivtsov et al., 2006; Wang et al., 2010).

Enrichment of human CML-related genes indicated convergence of BCR-ABL with Wnt/β-catenin and *Irf8* signaling in disease progression. Within the group of deregulated genes, we found association with enhanced glycolysis in accordance with gene expression analysis in human CML BP (A et al., 2010). Interestingly, leukemic GMPs also show up-regulation of *Hif1α*, as a potential cause of metabolic reprogramming (Zhao et al., 2010). This phenomenon is related to the Warburg effect and is considered as one of the most fundamental metabolic changes that occur during malignant transformation. Activated VEGF, insulin, and MAPK pathways (which are partially overlapping) were also evident. Many reports have documented a role of insulin as well as *Igf1* in a variety of cancers to provide antiapoptotic and proliferation stimuli (Pollak, 2008).

Growing evidence suggests that resistance to BCR-ABL inhibition involves increased drug export and/or altered intracellular signaling (Raaijmakers, 2007; Corrêa et al., 2012). Both mechanisms can be mediated by the efflux transporters *Abcc4*, *Abcc5*, and *Abcc11*, which are involved in discharging endogenous signaling molecules and nucleoside analogues. It has previously been shown that Wnt/β-catenin directly regulates *ABCB1* transporter gene transcription in CML and other malignancies (Corrêa et al., 2012; Stein et al., 2012), and that enforced expression of *Irf8* antagonized BCR-ABL and overcame drug resistance (Burchert et al., 2004). It was therefore interesting to see that the leukemic GMP fraction displayed enhanced expression of the ABC superfamily of efflux pumps. ABC family transporters have been reported to be involved in active TKI efflux and TKI resistance (Zhou et al., 2001; Jordanides et al., 2006; Deenik et al., 2010). We were also able to show enrichment of SP population in double mutated GMPs. The SP phenotype might explain the resistance of a subpopulation of leukemic cells to chemotherapy and represent one of the putative cancer stem cell populations (Golebiewska et al., 2011). Additional genes involved in drug resistance include *Ptgs1/Cox1* and *Bcl6*, both of which were also up-regulated in the leukemic GMP from blast-crisis (Zhang et al., 2009; Duy et al., 2011; Hurtz et al., 2011).

Our data show that inhibition of the BCR-ABL kinase by Imatinib was effective in WT, less so in single mutant cells that

were either *Irf8*-deficient or expressing stabilized β-catenin, and without effect in cells that combined both lesions. The mechanisms of Imatinib resistance comprise acquisition of point mutations in the BCR-ABL kinase domain (Shah et al., 2004), BCR-ABL amplification (Gorre et al., 2001), variability in the amount and function of the drug efflux protein, or resistance that occurs by additional mutations at the level of LICs that are not fully understood. Our results suggest that *Irf8* deletion plus β-catenin activation is responsible for treatment resistance and survival of BCR-ABL CML-LICs. Moreover, we have shown here that Wnt/β-catenin pathways and *Irf8* deficiency cooperate to provide a higher degree of Imatinib resistance than the Wnt/β-catenin pathway alone. Before the introduction of Imatinib, IFN-α was widely used in CML treatment. Notably, IFN-α induced Irf8 in BCR-ABL–transformed cells and protected against CML development (Nardi et al., 2009). The exact mechanism of action of IFN-α in the treatment of CML patients has not been fully revealed; however, enhanced *Irf8* expression emerges as a likely candidate.

In summary, the analogy of the genetic mouse model and human myeloid leukemia let us to conclude that increasing the dosage of canonical Wnt signaling under *Irf8* decline leverages progression of the disease from chronic into a BP and results in accumulation of TKI-resistant LICs. We conclude that future therapeutic concepts may consider measures to elevate *Irf8* expression and/or to abrogate β-catenin activation in myeloid leukemogenesis, especially in the context of disease relapse.

MATERIALS AND METHODS

Mice and genotyping. MxCre transgenic (Kühn et al., 1995), *Irf8*$^{-/-}$ (Holtschke et al., 1996), and mouse strains possessing the floxed alleles of Exon3 of β-catenin, *Ctnnb1*$^{(Ex3)fl/fl}$ (Harada et al., 1999), as well as the β-catenin floxed allele *Ctnnb1*$^{fl/fl}$ (Huelsken et al., 2001) have been previously described. Mice were genotyped using PCR, and primer sequences have been previously described (Holtschke et al., 1996; Domen et al., 1998; Huelsken et al., 2001; Scheller et al., 2006). MxCre^{+}*Ctnnb1*$^{(Ex3)fl/fl}$, *Irf8*$^{-/-}$MxCre^{+}*Ctnnb1*$^{(Ex3)fl/fl}$, MxCre^{+}*Ctnnb1*$^{fl/fl}$, and *Irf8*$^{-/-}$ MxCre^{+}*Ctnnb1*$^{fl/fl}$ mice were backcrossed for at least eight generations to the C57BL/6 background for all experiments, and MxCre^{-} littermates were used as controls. Congenic B6.SJL-Ptprc^{a}Pep3^{b}/BoyJ (here called B6.SJL) mice were originally obtained from Charles River and used as recipients for BM cell transplantation. Imatinib mesylate (Enzo Life Sciences) was administrated to mice by oral gavage twice a day (2 × 100 mg/kg of body weight per day in water). All mice were maintained under specific pathogen-free animal facilities at the MDC/Charité. All animal experiments were approved by the Commission for Animal Experiments at the MDC and the Berlin Office of Health (LAGeSo). Survival curves were calculated by the method of Kaplan-Meier, and statistical analysis was performed using Prism (version 5.0; GraphPad Software).

Retroviruses and transduction of cells. MSCV-*Irf8*-IRES-GFP and chimeric MSCV-*Irf8*-ER^{T2}-IRES-GFP constructs were donations from D. Carstanjen (FMP, Berlin, Germany). MSCV-β-catΔGSK-IRES-GFP construct was a gift from T. Reya (Duke University, Durham NC) and p210*BCR-ABL*-IRES-GFP control was a gift from A. Burchert (UKGM, Marburg, Germany). MSCV-IRES-GFP (MIG) construct was used as a control. The retrovirus packaging cell line (Phoenix-gp cells) was obtained from American Type Culture Collection. Virus production and cell infection was performed as described previously (Scheller et al., 2006).

Mouse transplantation experiments and generation of CML model. Freshly isolated BM cells were injected (2×10^6 cells/mouse) through the tail vein into lethally irradiated (9.5–10 Gy total body irradiation, Cs-137 source) B6.SJL recipient mice. Primary recipient mice were maintained on Sulfadoxin/Trimethoprim drinking water (40/8 mg/kg as a 0.1% Borgal, 1 wk) and allowed to engraft for 6 wk before being used for analysis. Repopulation was determined every 4 wk after transplantation by collection of peripheral blood, erythrocyte lysis, and staining of CD45.1 (Ly5.1; recipient) versus CD45.2 (Ly5.2; donor) engraftment. β–Catenin deletion or β-catenin activation (excision of Exon3 in the β-catenin gene) was induced by three i.p. injections of 400 µg poly(I:C) (GE Healthcare) in PBS on days 0, 3, and 5. Analysis of mice or harvesting of BM cells were performed 10–14 d after the last poly(I:C) injection. In all experiments, recipients transplanted with MxCre$^-$ *Ctnnb1*$^{(Ex3)fl/+}$, *Irf8*$^{-/-}$MxCre$^-$*Ctnnb1*$^{(Ex3)fl/+}$, MxCre$^-$ *Ctnnb1*$^{fl/fl}$, or *Irf8*$^{-/-}$ MxCre$^-$*Ctnnb1*$^{fl/fl}$ BM cells were used as controls for nonspecific poly(I:C) effects. In all experiments with activated β-catenin, we used heterozygous inducible MxCre$^+$*Ctnnb1*$^{(Ex3)fl/+}$ mice because of the dominant effect from a single activated *Ctnnb1* allele. To validate excision efficiency, genomic DNA from blood or harvested cells was subjected to PCR, as previously described (Huelsken et al., 2001; Scheller et al., 2006).

For investigation of *Irf8* overexpression, magnetically enriched hematopoietic progenitor cells (HPCs) and HSCs from C57/BL6 mice were infected with a retroviral vector expressing 4-OHT–inducible *Irf8* (*Irf8*-ER^{T2}-MIEG3) or control construct (ER^{T2}-MIEG3) and injected (2×10^6/mouse, 12.3–15% GFP-positive cells) in lethally (9.5 Gy) irradiated C57/BL6 mice. *Irf8* overexpression was induced 5 and 7 wk after transplantation by i.p. injection of 4-OHT every day for 5 d, using 1 mg per mouse dissolved in 100 µl of corn oil. Mice were analyzed biweekly after transplantation for evaluation of GFP$^+$ cell expansion in peripheral blood.

To generate the BCR–ABL–inducible CML model, Lin$^-$ BM cells from *Irf8*$^{-/-}$MxCre$^+$*Ctnnb1*$^{(Ex3)fl/+}$, *Irf8*$^{-/-}$MxCre$^-$*Ctnnb1*$^{(Ex3)fl/+}$, *Irf8*$^{+/+}$MxCre$^+$ *Ctnnb1*$^{(Ex3)fl/+}$, and control littermate *Irf8*$^{+/+}$MxCre$^-$*Ctnnb1*$^{(Ex3)fl/+}$ mice were infected with p210*BCR-ABL*-IRES-GFP virus construct containing supernatant medium. GFP$^+$ 7-AAD–negative progenitors were sorted 48 h after infection and co-cultured with OP9 stromal cells plus stem cell factor (SCF), Flt–3–ligand, and IL-7 (R&D Systems) for an additional 21 d. After expansion, 5,000 sorted GFP$^+$c-Kit$^+$CD11b$^+$ cells were transplanted intravenously into lethally irradiated (9.5 Gy) congenic recipient mice, along with 5×10^5 normal BM cells from B6.SJL (Ly5.1$^+$) mice. β–Catenin activation was induced by three i.p. injections of 400 µg poly(I:C) every 2nd d as described above/earlier. For serial transplantations, GFP$^+$ CML-LICs (5,000 or 10,000) were collected and pooled from two to three BMT mice and transplanted into a second set of lethally irradiated congenic recipient mice, along with 5×10^5 normal BM cells from B6.SJL (Ly5.1$^+$) mice. Mice were monitored daily for cachexia, lethargy, and ruff coats and moribund mice were killed. Leukemia was determined in peripheral blood, BM, spleen, and peripheral organs by FACS and histological analysis.

In vitro co-culture and Imatinib treatment. BCR–ABL–transduced GFP$^+$c-Kit$^+$ cells were sorted from the BM of second BMT mice after poly(I:C) treatment and development of clinically evident blast crisis. 10^4 freshly isolated cells were co-cultured with OP9 stromal cells supplemented with SCF, Flt-3-ligand, and IL-7 (R&D Systems) in the presence or absence of 5 µM Imatinib for 5 d. Colony formation was assessed by plating 10^3 cells into semisolid medium (M3434). Individual colonies were scored at 5 d after plating, and total number of cells were harvested, counted, and frequency of GFP$^+$ cells analyzed by FACS.

Cells preparation, FACS analysis, sorting, and SP cell staining. BM cell suspensions were prepared by flushing femurs and tibias with PBS. Cell suspensions from organs (spleen, liver, lymph nodes, and thymus) were obtained using 70-µm cell strainers (Falcon; BD). Peripheral blood samples were obtained from the tail vein and collected in EDTA-coated tubes. The blood cell counts were performed with automated veterinary hematological counter ScilVet abc Plus+ (SCIL GmbH), with software optimized for mouse

blood parameters. Red blood cells were lysed on ice using hypotonic erythrocyte lysis buffer (Pharmlyse buffer; BD). Cell staining and sorting was performed using Pacific blue, FITC, PE, APC, PE-Cy5, PE-Cy7, APC-Cy7, or biotin-labeled monoclonal antibodies directed against CD45.1 (A20), CD45.2 (104), B220 (6B2), CD19 (1D3), IL-7Rα chain (SB/199), CD3 (KT31.1), CD4 (GK1.5), CD8 (53–6.7), CD25 (3C7), CD44 (IM7), DX5, Gr1 (RB6.8C5), Mac1/CD11b (M1/70), Ter119, CD71 (C2), CD41 (MWReg30), c-Kit (2B8), Sca-1 (E13-161-7), CD34 (RAM34), FcγRII/III (2.4G2), CD135/Flt-3 (A2F10.1), and CD150/Slam (TC15-12F12.2; BD and eBioscience).

Cells were analyzed with FACSCalibur, FACSCanto II, or LSR II or sorted using FACSAria (BD) flow cytometers. Nonspecific antibody binding was reduced by preincubation with unconjugated antibody to FcγRII/III (2.4G2). Dead cells were excluded by propidium iodide or 7-AAD staining. Cell staining was performed using monoclonal antibodies described in supplementary information. Lineage-negative BM fraction was prepared by labeling cell suspensions with a mixture of antibodies to CD3e, CD4, CD8a, CD19, B220, Gr1, Il-7Rα, and Tερ119. Lin$^+$ cells were partially removed by using magnetic bead depletion (sheep anti–rat IgG-conjugated Dynabeads; Invitrogen). The LSK fraction of the BM, enriched for HSCs and MPPs, was stained and defined as Lin$^-$Sca-1$^-$c-Kit$^+$), whereas the HPCs (defined as Lin$^-$Sca-1$^-$c-Kit$^+$) contain CMPs (defined as Lin$^-$Sca-1$^-$c-Kit$^+$CD34$^+$FcγR II/III^{lo}), GMPs (Lin$^-$Sca-1$^-$ c-Kit$^+$CD34$^+$FcγR II/III^{hi}), and MEPs (Lin$^-$Sca-1$^-$c-Kit$^+$CD34$^-$FcγR II/III$^-$; Iwasaki and Akashi, 2007). For Annexin V staining, freshly isolated BM cells were stained with appropriate antibody, washed in binding buffer, and incubated in the dark with Annexin V–FITC or –APC (BD) for 20 min at 4°C. For SP cell analyses were done exactly as previously described (Ergen et al., 2013). Data were analyzed using CellQuest or FlowJo (Tree Star).

Colony-forming assay. Colony assay in methylcellulose were performed using MethoCult GF M3434 (STEMCELL Technologies) supplemented with 50 ng/ml rmSCF, 10 ng/ml rmIL-3, 10 ng/ml rhIL-6, and 3 U/ml rhEpo. Fixed numbers (2×10^4 BM or 10^5 spleen cells/ml) were seeded in triplicate into 35 mm^2 Petri dishes and incubated at 37°C in a humidified atmosphere of 5% CO_2 in air. Individual colonies (defined by >100 cells) were scored at 5–7 d after plating. For serial replating assays, cells were replated at 1-wk intervals for five rounds. Two independent experiments in triplicates each were performed and the number of colonies was compared using a paired Student's *t* test.

For WT and/or Irf8$^{-/-}$ BM cells infected with MSCV-*Irf8*-IRES-eGFP (provided by D. Carstanjen), MSCV-β-catΔGSK-IRES-eGFP (provided by T. Reya) and control MIG construct, GFP$^+$ cells were first sorted and seeded in in methylcellulose cultures (M3434, STEMCELL Technologies) as described above. Two independent experiments in triplicates were performed.

Quantitative RT-PCR. Total RNA from cells was extracted using RNeasy mini or micro kit from (QIAGEN). cDNA was generated using a poly(dT) oligonucleotides and SuperScript II Reverse Transcription (SuperScript II kit; Invitrogen) or using the Revert Aid First Strand cDNA Synthesis kit (Fermentas) and amplified on a 7300 Real Time PCR System (Applied Biosystems) using TaqMan probes for Irf8. Gene expression was normalized to β–actin (ABI: 4352341E). Alternatively, qRT-PCR reactions were performed using Platinum–SYBR green (Invitrogen) mix on the LightCycler 2.0 (Roche) system according to the manufacturer's instructions. At least triplicate reactions were performed for each gene. Melting curve analysis was performed after each run to control for the nonspecific PCR products and primer dimers. Ct values were related to copy numbers using standard curves. For each gene examined, a specific PCR fragment was synthesized that was extended at least 20–30 bp upstream and downstream of the amplicon generated by the primers used for the qRT-PCR. Normalization was performed using β–actin as an internal control. Primers for quantitative RT-PCR are listed in Tables S1 and S2.

Protein analysis. Lineage-depleted BM cells were lysed in buffer A (10 mM Hepes, pH 7.5, 10 mM KCl, 0.1 mM EDTA, 0.1 mM EGTA, and 0.1% NP-40) and subfractionated into cytosolic and nuclear membrane fractions by

2252

β-catenin and *Irf8* in leukemia progression | Scheller et al.

centrifugation at 2,000 g for 1 min. Each fraction was loaded onto SDS-PAGE gel, blotted (PVDF membrane; Millipore), and detected by a monoclonal mouse anti–β-catenin (BD), monoclonal mouse anti–β-actin (Sigma-Aldrich), coupled with ECL detection system (GE Healthcare). For detection of Irf8, lineage-depleted BM cells expressing stabilized β-catenin were lysed with RIPA buffer and detected by immunoblotting with polyclonal goat antibody to mouse Irf8 (Santa Cruz Biotechnology, Inc.) and monoclonal antibody to mouse α-tubulin (Santa Cruz Biotechnology, Inc.).

Irf8 promoter analysis, cloning, and site–directed mutagenesis of Irf8 promoter constructs. Upstream mouse and human genomic sequences for Irf8 were obtained from the UCSC Genome Bioinformatics Site (http://genome.cse.ucsc.edu/). Sequences were aligned using mVISTA, a set of programs for comparing DNA sequences from two or more species, available at http://genome.lbl.gov/vista/index.shtml.

To investigate whether Wnt/β-catenin signaling is involved in the transcriptional regulation of Irf8, the promoter region of Irf8 was analyzed. Three consensus binding elements for Tcf/Lef1 (TBEs, CTTTGA and TCAAAG, respectively) were found in a region 1.8 kb upstream from transcriptional start site.

Irf8 promoter fragments were PCR amplified from mouse genomic DNA using a proofreading Polymerase (Pfu; Fermentas) and primers with SacI or HindIII overhangs. Digested and purified fragments were inserted into the pGL3 basic reporter vector (Promega). Amplified Irf8 promoter fragments were F1/F0 (−1710 to +33 bp), F2/F0 (−1582 to +33 bp), and F3/F0 (−1318 to +33 bp). Mutation of the −1370 kb Tcf binding site (CTTTGAT to CTTTGGC) of the F2/F0 Irf8 promoter fragment was introduced by site-directed mutagenesis (Quick change site-directed mutagenesis kit; Stratagene) essentially as recommended by the manufacturer.

Transient transfections and luciferase–reporter assays. 293T/17 cells were transfected in triplicates. In brief: 100 ng of the Irf8 promoter reporter construct, 500 ng of chimeric β-catenin/Lef1 expression plasmid (provided by J. Huelsken, EPFL, Lausanne, Switzerland), or an empty pcDNA3.1 control vector and 100 ng pcDNA3.1 β–galactosidase were transfected using Metafectene (Biontex) according to the manufacturer's instructions. After 48 h, the cells were lysed and subjected to luciferase assay. Cell lysis and luciferase assay were performed using the Dual luciferase reporter assay kit (Promega) and a Glomax 20/20 luminometer (Turner Designs) according to the manufacturers' instructions. Firefly luciferase expression was normalized to β-galactosidase activity.

EMSA. 293T cells were transfected with a pcDNA-Lef1-HA expression construct or a mock control. Nuclear extracts were prepared as previously described (Rosenbauer et al., 2006) and incubated with an α–^{32}P–labeled probe containing the Tcf binding motif or a mutated Tcf binding motif (CTTTGAT to CTTTGGC). For competition experiments, unlabeled oligonucleotides with the WT or mutated Tcf-binding motif (CTTTGAT to CTTTGGC) were used. Oligonucleotides containing a human Cyclin D1 Tcf-binding site or a mutated human Cyclin D1 Tcf site (CTTTGAT to CTTTGGC) served as control (include source of Cyclin D1 Oligos as Reference). For supershift experiments, an anti-HA antibody was added.

Histology and cytology. Tissues were fixed in 3.7% formalin, embedded in paraffin, sectioned at 5 μm, and stained with hematoxylin-eosin stain. Blood smears and cytocentrifuge preparations were stained in May-Grunwald-Giemsa for morphological assessment. Sections were analyzed using an Axiophot microscope (Carl Zeiss). Images were acquired using a AxioCam camera and AxioVision software (version 3.1; Carl Zeiss).

Microarray analysis and statistical procedures. Gene expression profiles were generated from sorted LSK and GMP cells from three independent pools of MxCre$^-$Ctnnb1$^{(Ex3)fl/+}$, Ctnnb1$^{(Ex3)Δ/+}$, Irf8$^{-/-}$Ctnnb1$^{(Ex3)fl/+}$, and Irf8$^{-/-}$Ctnnb1$^{(Ex3)Δ/+}$ BMCs using Mouse 430_2 chip arrays (MG-430 PM peg arrays; GeneChip; Affymetrix). For normalization, quality control, and

data analysis, we used the corresponding affy/limma package functions of the Bioconductor system. Raw microarray data from Affymetrix CEL files were normalized using RMA. Quality Control identified 0 outliers. For identification of differentially expressed genes, we fitted a linear model using limma. The fold change cutoff was set to |1.5|, and the multiple testing corrected (Benjamini-Hochberg) p-value cutoff was selected as 0.05. For functional analysis, we used GSEA v2.0 algorithm (http://www.broadinstitute.org/gsea) using the computed t-statistic from limma as preranking. Microarray data (PSS) were uploaded to the Gene Expression Omnibus under accession no. GSE49054, showing the list of 638 genes (EntrezID, 394 UP, 244 DN) that were up- and down-regulated in Irf8$^{-/-}$Ctnnb1$^{(Ex3)Δ/+}$ GMPs from BP as compared with control GMPs.

Gene expression profiles of CML patient samples have been described previously (Radich et al., 2006). The data were downloaded from GEO (GSE4170) and analyzed for expression of IRF8 and Wnt target genes (Roel Nusse, the Wnt Homepage) in BM and PB samples from 42 chronic, 17 accelerated, and 32 BP CML patients using R/Bioconductor. For preprocessing, quantile normalization was applied. We assessed the statistically significant difference between IRF8 expression in the chronic group (CP) and the progression group (BC+AP) with a moderated t test (limma, P < 0.05). The same procedure was applied to a set of genes involved in Wnt target genes. Here, we compared samples from the progression group (BP) with the samples from the chronic group (CP) based on their IRF8 expression status.

We computed statistical significance of experimental results using two-tailed paired or unpaired Student's t tests. A p-value of <0.05 was considered statistically significant and marked by an asterisk. Two asterisks represent p-values of <0.001, whereas three asterisks represent p-values of <0.0001.

Online supplemental material. Table S1 shows primers for RT-PCR. Table S2 shows primers for TaqMan. Online supplemental material is available at http://www.jem.org/cgi/content/full/jem.20130706/DC1.

REFERENCES

A, J., S. Qian, G. Wang, B. Yan, S. Zhang, Q. Huang, L. Ni, W. Zha, L. Liu, B. Cao, et al. 2010. Chronic myeloid leukemia patients sensitive and resistant to imatinib treatment show different metabolic responses. *PLoS ONE.* 5:e13186. http://dx.doi.org/10.1371/journal.pone.0013186

Aberle, H., A. Bauer, J. Stappert, A. Kispert, and R. Kemler. 1997. beta-catenin is a target for the ubiquitin-proteasome pathway. *EMBO J.* 16:3797–3804. http://dx.doi.org/10.1093/emboj/16.13.3797

Abrahamsson, A.E., I. Geron, J. Gotlib, K.H. Dao, C.F. Barroga, I.G. Newton, F.J. Giles, J. Durocher, R.S. Creusot, M. Karimi, et al. 2009. Glycogen synthase kinase 3beta missplicing contributes to leukemia stem cell generation. *Proc. Natl. Acad. Sci. USA.* 106:3925–3929. http://dx.doi.org/10.1073/pnas.0900189106

Baba, Y., K.P. Garrett, and P.W. Kincade. 2005. Constitutively active beta-catenin confers multilineage differentiation potential on lymphoid and myeloid progenitors. *Immunity.* 23:599–609. http://dx.doi.org/10.1016/j.immuni.2005.10.009

Bartram, C.R., A. de Klein, A. Hagemeijer, T. van Agthoven, A. Geurts van Kessel, D. Bootsma, G. Grosveld, M.A. Ferguson-Smith, T. Davies,

M. Stone, et al. 1983. Translocation of c-ab1 oncogene correlates with the presence of a Philadelphia chromosome in chronic myelocytic leukaemia. *Nature*. 306:277–280. http://dx.doi.org/10.1038/306277a0

Bonnet, D., and J.E. Dick. 1997. Human acute myeloid leukemia is organized as a hierarchy that originates from a primitive hematopoietic cell. *Nat. Med.* 3:730–737. http://dx.doi.org/10.1038/nm0797-730

Buesche, G., A. Ganser, B. Schlegelberger, N. von Neuhoff, D. Gadzicki, H. Hecker, O. Bock, B. Frye, and H. Kreipe. 2007. Marrow fibrosis and its relevance during imatinib treatment of chronic myeloid leukemia. *Leukemia*. 21:2420–2427. http://dx.doi.org/10.1038/sj.leu.2404917

Burchert, A., D. Cai, L.C. Hofbauer, M.K.R. Samuelsson, E.P. Slater, J. Duyster, M. Ritter, A. Hochhaus, R. Müller, M. Eilers, et al. 2004. Interferon consensus sequence binding protein (ICSBP; IRF-8) antagonizes BCR/ABL and down-regulates bcl-2. *Blood*. 103:3480–3489. http://dx.doi.org/10.1182/blood-2003-08-2970

Cobas, M., A. Wilson, B. Ernst, S.J. Mancini, H.R. MacDonald, R. Kemler, and F. Radtke. 2004. β-catenin is dispensable for hematopoiesis and lymphopoiesis. *J. Exp. Med.* 199:221–229. http://dx.doi.org/10.1084/jem.20031615

Corrêa, S., R. Binato, B. Du Rocher, M.T. Castelo-Branco, L. Pizzatti, and E. Abdelhay. 2012. Wnt/β-catenin pathway regulates ABCB1 transcription in chronic myeloid leukemia. *BMC Cancer*. 12:303. http://dx.doi.org/10.1186/1471-2407-12-303

Crews, L.A., and C.H. Jamieson. 2013. Selective elimination of leukemia stem cells: Hitting a moving target. *Cancer Lett.* 338:15–22. http://dx.doi.org/10.1016/j.canlet.2012.08.006

Deenik, W., B. van der Holt, J.J. Janssen, I.W. Chu, P.J. Valk, G.J. Ossenkoppele, I.P. van der Heiden, P. Sonneveld, R.H. van Schaik, and J.J. Cornelissen. 2010. Polymorphisms in the multidrug resistance gene MDR1 (ABCB1) predict for molecular resistance in patients with newly diagnosed chronic myeloid leukemia receiving high-dose imatinib. *Blood*. 116:6144–6145, author reply :6145–6146. http://dx.doi.org/10.1182/blood-2010-07-296954

Deng, M., and G.Q. Daley. 2001. Expression of interferon consensus sequence binding protein induces potent immunity against BCR/ABL–induced leukemia. *Blood*. 97:3491–3497. http://dx.doi.org/10.1182/blood.V97.11.3491

Diaz-Blanco, E., I. Bruns, F. Neumann, J.C. Fischer, T. Graef, M. Rosskopf, B. Brors, S. Pechtel, S. Bork, A. Koch, et al. 2007. Molecular signature of CD34(+) hematopoietic stem and progenitor cells of patients with CML in chronic phase. *Leukemia*. 21:494–504. http://dx.doi.org/10.1038/sj.leu.2404549

Domen, J., K.L. Gandy, and I.L. Weissman. 1998. Systemic overexpression of BCL-2 in the hematopoietic system protects transgenic mice from the consequences of lethal irradiation. *Blood*. 91:2272–2282.

Druker, B.J., F. Guilhot, S.G. O'Brien, I. Gathmann, H. Kantarjian, N. Gattermann, M.W. Deininger, R.T. Silver, J.M. Goldman, R.M. Stone, et al; IRIS Investigators. 2006. Five-year follow-up of patients receiving imatinib for chronic myeloid leukemia. *N. Engl. J. Med.* 355:2408–2417. http://dx.doi.org/10.1056/NEJMoa062867

Duy, C., C. Hurtz, S. Shojaee, L. Cerchietti, H. Geng, S. Swaminathan, L. Klemm, S.M. Kweon, R. Nahar, M. Braig, et al. 2011. BCL6 enables Ph+ acute lymphoblastic leukaemia cells to survive BCR–ABL1 kinase inhibition. *Nature*. 473:384–388. http://dx.doi.org/10.1038/nature09883

Eppert, K., K. Takenaka, E.R. Lechman, L. Waldron, B. Nilsson, P. van Galen, K.H. Metzeler, A. Poeppl, V. Ling, J. Beyene, et al. 2011. Stem cell gene expression programs influence clinical outcome in human leukemia. *Nat. Med.* 17:1086–1093. http://dx.doi.org/10.1038/nm.2415

Ergen, A.V., M. Jeong, K.K. Lin, G.A. Challen, and M.A. Goodell. 2013. Isolation and characterization of mouse side population cells. *Methods Mol. Biol.* 946:151–162. http://dx.doi.org/10.1007/978-1-62703-128-8_10

Fereshteh, M., T. Ito, J.J. Kovacs, C. Zhao, H.Y. Kwon, V. Tornini, T. Konuma, M. Chen, R.J. Lefkowitz, and T. Reya. 2012. β-Arrestin2 mediates the initiation and progression of myeloid leukemia. *Proc. Natl. Acad. Sci. USA*. 109:12532–12537. http://dx.doi.org/10.1073/pnas.1209815109

Fodde, R., R. Smits, and H. Clevers. 2001. APC, signal transduction and genetic instability in colorectal cancer. *Nat. Rev. Cancer*. 1:55–67. http://dx.doi.org/10.1038/35094067

Gabriele, L., J. Phung, J. Fukumoto, D. Segal, I.M. Wang, P. Giannakakou, N.A. Giese, K. Ozato, and H.C. Morse III. 1999. Regulation of apoptosis in myeloid cells by interferon consensus sequence-binding protein. *J. Exp. Med.* 190:411–421. http://dx.doi.org/10.1084/jem.190.3.411

Golebiewska, A., N.H. Brons, R. Bjerkvig, and S.P. Niclou. 2011. Critical appraisal of the side population assay in stem cell and cancer stem cell research. *Cell Stem Cell*. 8:136–147. http://dx.doi.org/10.1016/j.stem.2011.01.007

Gorre, M.E., M. Mohammed, K. Ellwood, N. Hsu, R. Paquette, P.N. Rao, and C.L. Sawyers. 2001. Clinical resistance to STI-571 cancer therapy caused by BCR-ABL gene mutation or amplification. *Science*. 293:876–880. http://dx.doi.org/10.1126/science.1062538

Gurevich, R.M., P.M. Rosten, M. Schwieger, C. Stocking, and R.K. Humphries. 2006. Retroviral integration site analysis identifies ICSBP as a collaborating tumor suppressor gene in NUP98-TOP1-induced leukemia. *Exp. Hematol.* 34:1191–1201. http://dx.doi.org/10.1016/j.exphem.2006.04.020

Hao, S.X., and R. Ren. 2000. Expression of interferon consensus sequence binding protein (ICSBP) is downregulated in Bcr-Abl-induced murine chronic myelogenous leukemia-like disease, and forced coexpression of ICSBP inhibits Bcr-Abl-induced myeloproliferative disorder. *Mol. Cell. Biol.* 20:1149–1161. http://dx.doi.org/10.1128/MCB.20.4.1149-1161.2000

Hara, T., M. Schwieger, R. Kazama, S. Okamoto, K. Minehata, M. Ziegler, J. Löhler, and C. Stocking. 2008. Acceleration of chronic myeloproliferation by enforced expression of Meis1 or Meis3 in Icsbp-deficient bone marrow cells. *Oncogene*. 27:3865–3869. http://dx.doi.org/10.1038/sj.onc.1211043

Harada, N., Y. Tamai, T. Ishikawa, B. Sauer, K. Takaku, M. Oshima, and M.M. Taketo. 1999. Intestinal polyposis in mice with a dominant stable mutation of the beta-catenin gene. *EMBO J.* 18:5931–5942. http://dx.doi.org/10.1093/emboj/18.21.5931

Heidel, F.H., L. Bullinger, Z. Feng, Z. Wang, T.A. Neff, L. Stein, D. Kalaitzidis, S.W. Lane, and S.A. Armstrong. 2012. Genetic and pharmacologic inhibition of β-catenin targets imatinib-resistant leukemia stem cells in CML. *Cell Stem Cell*. 10:412–424. http://dx.doi.org/10.1016/j.stem.2012.02.017

Holtschke, T., J. Löhler, Y. Kanno, T. Fehr, N. Giese, F. Rosenbauer, J. Lou, K.P. Knobeloch, L. Gabriele, J.F. Waring, et al. 1996. Immunodeficiency and chronic myelogenous leukemia-like syndrome in mice with a targeted mutation of the ICSBP gene. *Cell*. 87:307–317. http://dx.doi.org/10.1016/S0092-8674(00)81348-3

Hu, Y., Y. Chen, L. Douglas, and S. Li. 2009. beta-Catenin is essential for survival of leukemic stem cells insensitive to kinase inhibition in mice with BCR-ABL-induced chronic myeloid leukemia. *Leukemia*. 23:109–116. http://dx.doi.org/10.1038/leu.2008.262

Huang, W., W. Zhou, G. Saberwal, I. Konieczna, E. Horvath, E. Katsoulidis, L.C. Platanias, and E.A. Eklund. 2010. Interferon consensus sequence binding protein (ICSBP) decreases beta-catenin activity in myeloid cells by repressing GAS2 transcription. *Mol. Cell. Biol.* 30:4575–4594. http://dx.doi.org/10.1128/MCB.01595-09

Huelsken, J., R. Vogel, B. Erdmann, G. Cotsarelis, and W. Birchmeier. 2001. beta-Catenin controls hair follicle morphogenesis and stem cell differentiation in the skin. *Cell*. 105:533–545. http://dx.doi.org/10.1016/S0092-8674(01)00336-1

Hurtz, C., K. Hatzi, L. Cerchietti, M. Braig, E. Park, Y.M. Kim, S. Herzog, P. Ramezani-Rad, H. Jumaa, M.C. Müller, et al. 2011. BCL6-mediated repression of p53 is critical for leukemia stem cell survival in chronic myeloid leukemia. *J. Exp. Med.* 208:2163–2174. http://dx.doi.org/10.1084/jem.20110304

Iwasaki, H., and K. Akashi. 2007. Hematopoietic developmental pathways: on cellular basis. *Oncogene*. 26:6687–6696. http://dx.doi.org/10.1038/sj.onc.1210754

Jamieson, C.H.M., L.E. Ailles, S.J. Dylla, M. Muijtjens, C. Jones, J.L. Zehnder, J. Gotlib, K. Li, M.G. Manz, A. Keating, et al. 2004. Granulocyte-macrophage progenitors as candidate leukemic stem cells in blast-crisis CML. *N. Engl. J. Med.* 351:657–667. http://dx.doi.org/10.1056/NEJMoa040258

Jeannet, G., M. Scheller, L. Scarpellino, S. Duboux, N. Gardiol, J. Back, F. Kuttler, I. Malanchi, W. Birchmeier, A. Leutz, et al. 2008. Long-term,

2254

β-catenin and *Irf8* in leukemia progression | Scheller et al.

multilineage hematopoiesis occurs in the combined absence of beta-catenin and gamma-catenin. *Blood*. 111:142–149. http://dx.doi.org/10.1182/blood-2007-07-102558

Jordanides, N.E., H.G. Jorgensen, T.L. Holyoake, and J.C. Mountford. 2006. Functional ABCG2 is overexpressed on primary CML CD34+ cells and is inhibited by imatinib mesylate. *Blood*. 108:1370–1373. http://dx.doi.org/10.1182/blood-2006-02-003145

Kim, K., K.M. Pang, M. Evans, and E.D. Hay. 2000. Overexpression of beta-catenin induces apoptosis independent of its transactivation function with LEF-1 or the involvement of major G1 cell cycle regulators. *Mol. Biol. Cell*. 11:3509–3523. http://dx.doi.org/10.1091/mbc.11.10.3509

Kirstetter, P., K. Anderson, B.T. Porse, S.E. Jacobsen, and C. Nerlov. 2006. Activation of the canonical Wnt pathway leads to loss of hematopoietic stem cell repopulation and multilineage differentiation block. *Nat. Immunol*. 7:1048–1056. http://dx.doi.org/10.1038/ni1381

Kirstetter, P., M.B. Schuster, O. Bereshchenko, S. Moore, H. Dvinge, E. Kurz, K. Theilgaard-Mönch, R. Månsson, T.A. Pedersen, T. Pabst, et al. 2008. Modeling of C/EBPalpha mutant acute myeloid leukemia reveals a common expression signature of committed myeloid leukemia-initiating cells. *Cancer Cell*. 13:299–310. http://dx.doi.org/10.1016/j.ccr.2008.02.008

Koch, U., A. Wilson, M. Cobas, R. Kemler, H.R. Macdonald, and F. Radtke. 2008. Simultaneous loss of beta- and gamma-catenin does not perturb hematopoiesis or lymphopoiesis. *Blood*. 111:160–164. http://dx.doi.org/10.1182/blood-2007-07-099754

Koenigsmann, J., and D. Carstanjen. 2009. Loss of Irf8 does not co-operate with overexpression of BCL-2 in the induction of leukemias in vivo. *Leuk. Lymphoma*. 50:2078–2082. http://dx.doi.org/10.3109/10428190903296913

Krivtsov, A.V., D. Twomey, Z. Feng, M.C. Stubbs, Y. Wang, J. Faber, J.E. Levine, J. Wang, W.C. Hahn, D.G. Gilliland, et al. 2006. Transformation from committed progenitor to leukaemia stem cell initiated by MLL-AF9. *Nature*. 442:818–822. http://dx.doi.org/10.1038/nature04980

Kubosaki, A., G. Lindgren, M. Tagami, C. Simon, Y. Tomaru, H. Miura, T. Suzuki, E. Arner, A.R. Forrest, K.M. Irvine, et al. 2010. The combination of gene perturbation assay and ChIP-chip reveals functional direct target genes for IRF8 in THP-1 cells. *Mol. Immunol*. 47:2295–2302. http://dx.doi.org/10.1016/j.molimm.2010.05.289

Kühn, R., F. Schwenk, M. Aguet, and K. Rajewsky. 1995. Inducible gene targeting in mice. *Science*. 269:1427–1429. http://dx.doi.org/10.1126/science.7660125

Lane, S.W., Y.J. Wang, C. Lo Celso, C. Ragu, L. Bullinger, S.M. Sykes, F. Ferraro, S. Shterental, C.P. Lin, D.G. Gilliland, et al. 2011. Differential niche and Wnt requirements during acute myeloid leukemia progression. *Blood*. 118:2849–2856. http://dx.doi.org/10.1182/blood-2011-03-345165

Li, S., R.L. Ilaria Jr., R.P. Million, G.Q. Daley, and R.A. Van Etten. 1999. The P190, P210, and P230 forms of the BCR/ABL oncogene induce a similar chronic myeloid leukemia-like syndrome in mice but have different lymphoid leukemogenic activity. *J. Exp. Med*. 189:1399–1412. http://dx.doi.org/10.1084/jem.189.9.1399

Luis, T.C., B.A. Naber, P.P. Roozen, M.H. Brugman, E.F. de Haas, M. Ghazvini, W.E. Fibbe, J.J. van Dongen, R. Fodde, and F.J. Staal. 2011. Canonical wnt signaling regulates hematopoiesis in a dosage-dependent fashion. *Cell Stem Cell*. 9:345–356. http://dx.doi.org/10.1016/j.stem.2011.07.017

Luis, T.C., N.M. Killmann, and F.J. Staal. 2012. Signal transduction pathways regulating hematopoietic stem cell biology: introduction to a series of Spotlight Reviews. *Leukemia*. 26:86–90. http://dx.doi.org/10.1038/leu.2011.260

Malhotra, S., and P.W. Kincade. 2009. Wnt-related molecules and signaling pathway equilibrium in hematopoiesis. *Cell Stem Cell*. 4:27–36. http://dx.doi.org/10.1016/j.stem.2008.12.004

Månsson, R., A. Hultquist, S. Luc, L. Yang, K. Anderson, S. Kharazi, S. Al-Hashmi, K. Liuba, L. Thorén, J. Adolfsson, et al. 2007. Molecular evidence for hierarchical transcriptional lineage priming in fetal and adult stem cells and multipotent progenitors. *Immunity*. 26:407–419. http://dx.doi.org/10.1016/j.immuni.2007.02.013

Müller-Tidow, C., B. Steffen, T. Cauvet, L. Tickenbrock, P. Ji, S. Diederichs, B. Sargin, G. Köhler, M. Stelljes, E. Puccetti, et al. 2004. Translocation products in acute myeloid leukemia activate the Wnt signaling pathway in hematopoietic cells. *Mol. Cell. Biol*. 24:2890–2904. http://dx.doi.org/10.1128/MCB.24.7.2890-2904.2004

Nardi, V., O. Naveiras, M. Azam, and G.Q. Daley. 2009. ICSBP-mediated immune protection against BCR–ABL-induced leukemia requires the CCL6 and CCL9 chemokines. *Blood*. 113:3813–3820. http://dx.doi.org/10.1182/blood-2008-07-167189

Nowell, P.C., and D.A. Hungerford. 1960. Chromosome studies on normal and leukemic human leukocytes. *J. Natl. Cancer Inst*. 25:85–109.

Oehler, V.G., K.Y. Yeung, Y.E. Choi, R.E. Bumgarner, A.E. Raftery, and J.P. Radich. 2009. The derivation of diagnostic markers of chronic myeloid leukemia progression from microarray data. *Blood*. 114:3292–3298. http://dx.doi.org/10.1182/blood-2009-03-212969

Perrotti, D., C. Jamieson, J. Goldman, and T. Skorski. 2010. Chronic myeloid leukemia: mechanisms of blastic transformation. *J. Clin. Invest*. 120:2254–2264. http://dx.doi.org/10.1172/JCI41246

Perry, J.M., X.C. He, R. Sugimura, J.C. Grindley, J.S. Haug, S. Ding, and L. Li. 2011. Cooperation between both Wnt/beta-catenin and PTEN/PI3K/Akt signaling promotes primitive hematopoietic stem cell self-renewal and expansion. *Genes Dev*. 25:1928–1942. http://dx.doi.org/10.1101/gad.17421911

Pollak, M. 2008. Insulin and insulin-like growth factor signalling in neoplasia. *Nat. Rev. Cancer*. 8:915–928. http://dx.doi.org/10.1038/nrc2536

Raaijmakers, M.H. 2007. ATP-binding-cassette transporters in hematopoietic stem cells and their utility as therapeutic targets in acute and chronic myeloid leukemia. *Leukemia*. 21:2094–2102. http://dx.doi.org/10.1038/sj.leu.2404859

Radich, J.P., H. Dai, M. Mao, V. Oehler, J. Schelter, B. Druker, C. Sawyers, N. Shah, W. Stock, C.L. Willman, et al. 2006. Gene expression changes associated with progression and response in chronic myeloid leukemia. *Proc. Natl. Acad. Sci. USA*. 103:2794–2799. http://dx.doi.org/10.1073/pnas.0510423103

Reya, T., A.W. Duncan, L. Ailles, J. Domen, D.C. Scherer, K. Willert, L. Hintz, R. Nusse, and I.L. Weissman. 2003. A role for Wnt signalling in self-renewal of haematopoietic stem cells. *Nature*. 423:409–414. http://dx.doi.org/10.1038/nature01593

Rosenbauer, F., and D.G. Tenen. 2007. Transcription factors in myeloid development: balancing differentiation with transformation. *Nat. Rev. Immunol*. 7:105–117. http://dx.doi.org/10.1038/nri2024

Rosenbauer, F., B.M. Owens, L. Yu, J.R. Tumang, U. Steidl, J.L. Kutok, L.K. Clayton, K. Wagner, K. Scheller, H. Iwasaki, et al. 2006. Lymphoid cell growth and transformation are suppressed by a key regulatory element of the gene encoding PU.1. *Nat. Genet*. 38:27–37. http://dx.doi.org/10.1038/ng1679

Scheller, M., J. Foerster, C.M. Heyworth, J.F. Waring, J. Löhler, G.L. Gilmore, R.K. Shadduck, T.M. Dexter, and I. Horak. 1999. Altered development and cytokine responses of myeloid progenitors in the absence of transcription factor, interferon consensus sequence binding protein. *Blood*. 94:3764–3771.

Scheller, M., J. Huelsken, F. Rosenbauer, M.M. Taketo, W. Birchmeier, D.G. Tenen, and A. Leutz. 2006. Hematopoietic stem cell and multilineage defects generated by constitutive beta-catenin activation. *Nat. Immunol*. 7:1037–1047. http://dx.doi.org/10.1038/ni1387

Schmidt, M., S. Nagel, J. Proba, C. Thiede, M. Ritter, J.F. Waring, F. Rosenbauer, D. Huhn, B. Wittig, I. Horak, and A. Neubauer. 1998. Lack of interferon consensus sequence binding protein (ICSBP) transcripts in human myeloid leukemias. *Blood*. 91:22–29.

Schmidt, M., A. Hochhaus, A. Nitsche, R. Hehlmann, and A. Neubauer. 2001. Expression of nuclear transcription factor interferon consensus sequence binding protein in chronic myeloid leukemia correlates with pretreatment risk features and cytogenetic response to interferon-alpha. *Blood*. 97:3648–3650. http://dx.doi.org/10.1182/blood.V97.11.3648

Schwieger, M., J. Löhler, J. Friel, M. Scheller, I. Horak, and C. Stocking. 2002. AML1-ETO inhibits maturation of multiple lymphohematopoietic lineages and induces myeloblast transformation in synergy with ICSBP deficiency. *J. Exp. Med*. 196:1227–1240. http://dx.doi.org/10.1084/jem.20020824

Shah, N.P., C. Tran, F.Y. Lee, P. Chen, D. Norris, and C.L. Sawyers. 2004. Overriding imatinib resistance with a novel ABL kinase inhibitor. *Science*. 305:399–401. http://dx.doi.org/10.1126/science.1099480

Shtutman, M., J. Zhurinsky, I. Simcha, C. Albanese, M. D'Amico, R. Pestell, and A. Ben-Ze'ev. 1999. The cyclin D1 gene is a target of the beta-catenin/LEF-1 pathway. *Proc. Natl. Acad. Sci. USA*. 96:5522–5527. http://dx.doi.org/10.1073/pnas.96.10.5522

Stein, U., C. Fleuter, F. Siegel, J. Smith, A. Kopacek, D.A. Scudiero, K.M. Hite, P.M. Schlag, R.H. Shoemaker, and W. Walther. 2012. Impact of mutant β-catenin on ABCB1 expression and therapy response in colon cancer cells. *Br. J. Cancer*. 106:1395–1405. http://dx.doi.org/10.1038/bjc.2012.81

Tamura, T., H.J. Kong, C. Tunyaplin, H. Tsujimura, K. Calame, and K. Ozato. 2003. ICSBP/IRF-8 inhibits mitogenic activity of p210 Bcr/Abl in differentiating myeloid progenitor cells. *Blood*. 102:4547–4554. http://dx.doi.org/10.1182/blood-2003-01-0291

Tamura, T., P. Thotakura, T.S. Tanaka, M.S.H. Ko, and K. Ozato. 2005. Identification of target genes and a unique cis element regulated by IRF-8 in developing macrophages. *Blood*. 106:1938–1947. http://dx.doi.org/10.1182/blood-2005-01-0080

Wang, Y., A.V. Krivtsov, A.U. Sinha, T.E. North, W. Goessling, Z. Feng, L.I. Zon, and S.A. Armstrong. 2010. The Wnt/beta-catenin pathway is required for the development of leukemia stem cells in AML. *Science*. 327:1650–1653. http://dx.doi.org/10.1126/science.1186624

Yeung, J., M.T. Esposito, A. Gandillet, B.B. Zeisig, E. Griessinger, D. Bonnet, and C.W.E. So. 2010. β-Catenin mediates the establishment and drug resistance of MLL leukemic stem cells. *Cancer Cell*. 18:606–618. http://dx.doi.org/10.1016/j.ccr.2010.10.032

Zhang, W.W., J.E. Cortes, H. Yao, L. Zhang, N.G. Reddy, E. Jabbour, H.M. Kantarjian, and D. Jones. 2009. Predictors of primary imatinib resistance in chronic myelogenous leukemia are distinct from those in secondary imatinib resistance. *J. Clin. Oncol*. 27:3642–3649. http://dx.doi.org/10.1200/JCO.2008.19.4076

Zhao, C., J. Blum, A. Chen, H.Y. Kwon, S.H. Jung, J.M. Cook, A. Lagoo, and T. Reya. 2007. Loss of beta-catenin impairs the renewal of normal and CML stem cells in vivo. *Cancer Cell*. 12:528–541. http://dx.doi.org/10.1016/j.ccr.2007.11.003

Zhao, F., A. Mancuso, T.V. Bui, X. Tong, J.J. Gruber, C.R. Swider, P.V. Sanchez, J.J. Lum, N. Sayed, J.V. Melo, et al. 2010. Imatinib resistance associated with BCR–ABL upregulation is dependent on HIF-1alpha-induced metabolic reprograming. *Oncogene*. 29:2962–2972. http://dx.doi.org/10.1038/onc.2010.67

Zheng, C., L. Li, M. Haak, B. Brors, O. Frank, M. Giehl, A. Fabarius, M. Schatz, A. Weisser, C. Lorentz, et al. 2006. Gene expression profiling of CD34+ cells identifies a molecular signature of chronic myeloid leukemia blast crisis. *Leukemia*. 20:1028–1034. http://dx.doi.org/10.1038/sj.leu.2404227

Zhou, S., J.D. Schuetz, K.D. Bunting, A.M. Colapietro, J. Sampath, J.J. Morris, I. Lagutina, G.C. Grosveld, M. Osawa, H. Nakauchi, and B.P. Sorrentino. 2001. The ABC transporter Bcrp1/ABCG2 is expressed in a wide variety of stem cells and is a molecular determinant of the side-population phenotype. *Nat. Med*. 7:1028–1034. http://dx.doi.org/10.1038/nm0901-1028